



final report

Project code: B.FLT.0374

Prepared by: David Gobbett, Steven Crimp and Garry Hopwood
CSIRO Agriculture Flagship

Date published: 28 November 2014

PUBLISHED BY
Meat and Livestock Australia Limited
PO Box 1961
NORTH SYDNEY NSW 2059

Understanding the changing nature of heat stress in Australian feedlots

Meat & Livestock Australia acknowledges the matching funds provided by the Australian Government to support the research and development detailed in this publication.

This publication is published by Meat & Livestock Australia Limited ABN 39 081 678 364 (MLA). Care is taken to ensure the accuracy of the information contained in this publication. However MLA cannot accept responsibility for the accuracy or completeness of the information or opinions contained in the publication. You should make your own enquiries before making decisions concerning your interests. Reproduction in whole or in part of this publication is prohibited without prior written consent of MLA.

Abstract

The heat load index (HLI) and accumulated heat load units (AHLU) are calculated from weather data and used by the livestock industry to assess heat stress impacts on cattle. This work examined the changing nature of heat stress using these metrics both historically and in the future, for five major feedlot regions of Australia. Changes in heat stress over the five decades from 1963 to 2012, as well as changes for future years 2030 and 2050 have been evaluated and are presented in this report.

The historical analyses show wide ranges in heat stress levels between regions, with central Queensland experiencing the most heat related stress (37 high risk days per year for sensitive cattle) and southwest WA experiencing the least (4.2 days per year). The scenarios for the future years vary considerably between the regions. The number of annual high heat stress days affecting highly sensitive cattle in central Queensland may increase 6-13% by 2030 and 16-19% by 2050. Southwest WA is projected to experience lower increases in high heat stress days (for highly susceptible cattle) with a 7-10% increase in 2030 but a 15-19% increase by 2050.

Various management options exist to reduce heat stress, or to enhance the cattle tolerance, and understanding the historical trends and likely future scenarios of heat stress will inform future feedlot management strategies.

Executive summary

Heat stress is a significant issue for livestock enterprises and particularly feedlots. The detrimental effects of heat stress on livestock result in significant loss of income and increases in management costs, and are also an animal welfare concern. The economic impacts of heat stress have been estimated to cost the Australian feedlot industry in excess of \$16.5 M annually¹.

The heat load index (HLI)² is used by the livestock industry to assess heat stress impacts on cattle. The HLI is calculated from meteorological data, including air temperature, solar radiation, humidity and wind speed, but is not a direct measurement of heat stress impact on cattle. Heat stressed cattle accumulate heat load, with body temperature rising during the day and then reducing as heat is dissipated during cooler night-time conditions. However, if overnight cooling is not adequate to compensate for the heat load acquired during the previous day, an accumulation of heat load occurs². Accumulated heat load units (AHLU)³ can be calculated from the HLI at different times of day. Heat stress categorised using AHLU relates to panting scores in cattle as shown in Table 1.

Table 1: Heat stress categories based on AHLU^{2,4} with corresponding cattle panting scores.

AHLU	Heat stress category	Panting score
0-20	Low risk	1 (or no stress)
20-50	Medium risk	1 – 2
50-100	High risk	2 – 4
> 100	Extreme risk	4

Gaughan *et al.*⁸ introduced the HLI and estimated the upper HLI threshold at which cattle will start to accumulate heat load. Many factors influence the degree of heat stress experienced by cattle and influence the threshold HLI above which heat load is accumulated. These factors include genotype, coat colour, health status, degree of acclimatization, access to shade and time spent on feed. For example, British *Bos taurus* cattle exhibit an upper threshold of 86, whereas purebred *Bos indicus* have much higher upper threshold of 96 (or possibly higher). In feedlots, management factors such as removal of wet manure, provision of shade, drinking water temperature, as well as the type of feed and timing of feeding can also affect the ability of cattle to tolerate heat stress⁵.

The aim of this research is to develop an understanding of the changing nature of heat stress at both seasonal and decadal scales for five case study regions in Australia. The two broad objectives of this work were to calculate and summarise heat load indices (HLI and AHLU) for the five major Australian regions where feedlots are located, which are central Queensland (CQ), southern Queensland (SEQ), northern New South Wales (NNSW), Riverina (RIV) and southwest Western Australia (SWA):

- Using historical climate surface data to quantify the changes in frequency and duration of heat stress events over the period 1963 to 2012.

¹ Sackett, D., P. Holmes, K. Abbott, S. Jephcott & M. Barber. 2006. Assessing the economic cost of endemic disease on the profitability of Australian beef cattle and sheep producers. AHW.087. North Sydney NSW.

² Gaughan, J. B., T. L. Mader, S. M. Holt & A. Lisle (2008) A new heat load index for feedlot cattle. *Journal of Animal Science*, 86, 226-234.

³ Meat and Livestock Australia. 2006. Tips and tools: Heat load in feedlot cattle. North Sydney: Meat and Livestock Australia.

⁴ Katestone Environmental. 2011. FLOT.334 Cattle Heat Load Forecast Service for 2005/2006 Summer. 56. MLA, North Sydney, NSW

⁵ Kennedy, P. & P. Cronjé. 2005. FLOT.314 - Dietary strategies for amelioration of heat load in feedlot cattle Meat & Livestock Australia Limited.

- Use global climate models (GCMs) to project the future changes in frequency and duration of heat stress events for 2030 and 2050.

HLI was calculated and summarised using the AHLU (in the categories shown in Table 1), for cattle with high sensitivity and lower sensitivity (HLI thresholds of 86 and 96 respectively) using gridded climate datasets with a grid size of approximately 5 km. AHLU was summarised in terms of the mean number of days per year in each risk category, and the mean duration of periods with risk levels in (or above) each risk category.

Key findings from the historical analysis were that across the five regions, CQ experienced the highest level of heat stress, SEQ and NNSW lower levels, RIV less again and SWA the lowest. Summaries for the high risk category (AHLU > 50) are shown in Table 2. Unsurprisingly, fewer heat stress days and shorter periods of heat stress periods were calculated for lower sensitivity cattle (using a higher HLI threshold of 96). Detailed regional summary statistics are presented in Appendix 1, with tables of the number of days per year for the high sensitivity (Table 8) and low sensitivity classes of cattle (Table 9), and mean duration of heat stress periods for high sensitivity (Table 10) and low sensitivity cattle (Table 11). For highly susceptible cattle (HLI threshold of 86), the annual trends (1975 to 2012) in high and extreme heat stress, show an increasing trend in all regions. For less susceptible cattle, the trends figures show no significant increase to some increases in the five regions.

Table 2: Summary of the number of high heat stress (AHLU > 50) days of annually and the mean duration of those periods for two classes of cattle sensitivity, for the five feedlot regions.

Region	High sensitivity cattle (HLI 86)		Low sensitivity cattle (HLI 96)	
	Mean number of days/year	Mean duration (days)	Mean number of days/year	Mean duration (days)
CQ	37.4	3.2	0.1	0.4
SEQ	16.9	2.1	0.0	0.1
NNSW	14.5	2.1	0.1	0.3
RIV	9.3	1.8	0.1	0.5
SWA	4.2	1.3	0.0	0.1

Maps of the historical decadal heat stress patterns have been produced (Figure 5 through Figure 24, Appendix 3) show the mean number of heat stress days per year, and average duration of heat stress periods, in each of 4 AHLU classes.

Across all of the five sites, increasing trends in the duration of heat stress events were observed for AHLU classes >1, >20 and in some instances >50. These increasing trends were most pronounced in Central Queensland and Northern NSW regions (See Appendix 3).

To assess likely patterns of heat stress in the future, four global climate models (GCMs) were selected which have been assessed as adequately simulating the El Niño Southern Oscillation (ENSO) which is an important component of Australia's climatic variability. HLI and AHLU were calculated using the data from these four models, for a baseline period (1975 to 2012) and comparing that with HLI calculated for two twenty year periods centred on 2030 (2020 to 2040) and 2050 (2040 to 2060). By comparing the baseline and future scenarios, a percentage increase in AHLU was able to be derived for each of the four models, for the future scenario years.

The range of increases in high heat stress predicted for 2030 by the four models is presented in Table 3. These results suggest that those regions which currently experience higher levels of heat stress will, in general, experience greater increases in future. The 2030 scenario for CQ showed a 14-

80% increase in duration of high heat stress periods for highly sensitive cattle, and a 23-39% increase for lower sensitivity cattle. The scenarios for the SWA region showed a 5-17% increase and 4-13% increase in duration for high and lower sensitivity cattle respectively for 2030. Detailed tabulated results are presented in Table 12 to Table 15 (Appendix 2) and maps have been produced for the five regions, showing changes in AHLU predicted using each of the four models (Figure 25 to Figure 64 in Appendix 4).

Table 3: Range of predicted changes, under four GCM scenarios for 2030, in the number of high heat stress (AHLU > 50) days annually and the mean duration of those periods, for two classes of cattle sensitivity.

Region	High sensitivity cattle		Low sensitivity cattle	
	Percent increase in number of days/year	Percent increase in mean duration (days)	Percent increase in mean number of days/year	Percent increase in mean duration (days)
CQ	6 – 13	14 – 80	11 – 18	23 – 39
SEQ	7 – 14	8 – 32	12 – 30	10 – 32
NNSW	5 – 13	5 – 33	13 – 30	10 – 34
RIV	7 – 16	5 – 33	14 - 33	8 – 29
SWA	7 - 10	5 - 17	11 - 17	4 - 13

The results from this analyses show that both the frequency and duration of heat stress events will increase in the future, with ambient temperature conditions less conducive the heat shedding at night. This would suggest that the management of feedlot heat stress will become more challenging in the future particularly in both Central Queensland and Northern NSW regions. This may mean that in these regions changes in the design of shade infrastructure, feed, water and waste management may need to change^{6,7}. Livestock producers can mitigate heat stress with shade structures, cooling systems, or altered feed, but these methods increase production and capital costs

⁶ Gaughan, J., N. Lacetera, S. E. Valtorta, H. H. Khalifa, L. Hahn & T. Mader. 2009. Response of domestic animals to climate challenges. In *Biometeorology for adaptation to climate variability and change*, 131-170. Springer.

⁷ Nidumolu, U. B., S. Crimp, D. Gobbett, A. Laing & S. Little (2010) Heat stress in dairy cattle in northern Victoria: responses to a changing climate. *CSIRO Climate Adaptation Flagship Working Paper No. 10*. <http://www.csiro.au/Organisation-Structure/Flagships/Climate-Adaptation-Flagship/CAF-working-papers/CAF-working-paper-10.aspx> (last accessed 19th Nov 2014).

Table of contents

1	Background	7
2	Project objectives.....	8
3	Methodology	9
3.1	Study regions.....	9
3.2	Historic analyses.....	10
3.2.1	Input datasets.....	10
3.2.2	Solar Irradiance.....	10
3.2.3	Black globe temperature	11
3.2.4	Relative humidity.....	12
3.2.5	Wind speed.....	12
3.2.6	Calculation of HLI.....	12
3.2.7	Calculation of AHLU	13
3.2.8	Summarising heat stress.....	14
3.3	Climate scenario analyses.....	14
3.3.1	Methods.....	14
3.3.2	Black globe temperature	17
3.3.3	Relative humidity.....	17
3.3.4	Wind speed.....	17
3.3.5	Calculation of HLI and AHLU	18
4	Results	18
4.1	Historical analysis	18
4.2	AHLU under future scenarios	20
5	Discussion and conclusions.....	21
6	Bibliography.....	24
7	Acknowledgements.....	26
Appendix 1 – Summaries of historical heat stress		27
Appendix 2 – Summaries of future scenario heat stress		30
Appendix 3 – Maps of historical heat stress.....		34
Appendix 4 – Maps of future scenario heat stress.....		44

1 Background

The Heat Load Index⁸ (HLI) is an established index used by the cattle industry for assessing and predicting heat stress impacts. Additionally, Accumulated Heat Load Units^{2,9} (AHLU) are a secondary index which is based on the HLI, and which models the accumulation and dissipation of heat load by cattle over time. HLI and AHLU are calculated from sub-daily meteorological data, including air temperature, solar radiation, humidity and wind speed. HLI is therefore not a direct measurement of impacts on cattle, so may not fully represent all the factors that influence the degree of heat stress experienced by cattle.

Gaughan *et al.*⁸ introduced the HLI and highlighted several factors which influence the upper HLI threshold at which cattle will start to accumulate heat load. Cattle genotype is an important factor with, for example, British *Bos taurus* cattle exhibiting an upper threshold of 86, whereas pure-bred *Bos indicus* have a much higher upper threshold of 96 (or possibly higher). Additionally, cattle coat colour, health status, acclimatisation, age and time spent on feed can also impact the threshold at which heat load starts to accumulate. In feedlots, management factors such as removal of wet manure, provision of shade, drinking water temperature, and type/timing of feeding can also affect the ability of cattle to tolerate heat stress¹⁰.

Gridded historical climate datasets are available which cover Australia at a spatial scale of 0.05° of latitude and longitude (approximately a 5 km grid)^{11,12}, and provide a valuable basis for examining climatic trends over recent decades, the generation of climatic indices (such as the HLI and AHLU), to provide strategic information to livestock industries about heat stress. Such indices include the temperature humidity index¹³ (THI), HLI and AHLU. At this scale gridded climate data are only available to be able to estimate HLI twice per day (at times of minimum and maximum temperature). This spatial and temporal scale is too broad to incorporate factors that influence climate at a local scale, or specific factors mentioned above which affect cattle sensitivity to heat stress. However, by applying consistent methods using these data, it is possible to make useful comparisons over time and between regions, as well as examine how heat stress events have changed in their magnitude and frequency over time.

Future climate change projections are generated by a number of state-of-the art global climate models (GCMs). These models provide credible simulations of future climatic conditions at spatial scales which may then be applied to historical climate data of 0.05° (approximately 5 km) grid resolution to allow calculation of HLI and AHLU under future climate scenarios in the same way as for the historical period.

⁸ Gaughan, J. B., T. L. Mader, S. M. Holt & A. Lisle (2008) A new heat load index for feedlot cattle. *Journal of Animal Science*, 86, 226-234.

⁹ Meat and Livestock Australia. 2006. Tips and tools: Heat load in feedlot cattle. North Sydney: Meat and Livestock Australia.

¹⁰ Kennedy, P. & P. Cronjé. 2005. FLOT.314 - Dietary strategies for amelioration of heat load in feedlot cattle Meat & Livestock Australia Limited.

¹¹ Jeffrey, S. J., J. O. Carter, K. B. Moodie & A. R. Beswick (2001) Using spatial interpolation to construct a comprehensive archive of Australian climate data. *Environmental Modelling & Software*, 16, 309-330.

¹² Jones, D. A., W. Wang & R. Fawcett (2009) High-quality spatial climate data-sets for Australia. *Australian Meteorological and Oceanographic Journal*, 58, 233-248.

¹³ Nidumolu, U., S. Crimp, D. Gobbett, A. Laing, M. Howden & S. Little (2014) Spatio-temporal modelling of heat stress and climate change implications for the Murray dairy region, Australia. *Int J Biometeorol*, 58, 1095-108.

2 Project objectives

The two broad objectives of this work were to calculate and summarise heat load indices (HLI and AHLU) for the five major regions where feedlots are located (central Queensland, southern Queensland, northern New South Wales, Riverina and southwest Western Australia):

1. Using historical climate surface data to quantify the changes in frequency and duration of heat stress events over the period 1963 to 2012.
2. Apply climate change scenarios to project the future changes in frequency and duration of heat stress events for 2030 and 2050.

3 Methodology

3.1 Study regions

As part of the initial scoping, five feedlot regions were defined (Figure 1) in central Queensland (CQ), south eastern Queensland (SEQ), northern New South Wales (NNSW), Riverina (RIV) and southwest Western Australia (SWA). Table 4 summarises the sizes of the regions which range in size from 90,326 km² to 121,829 km².

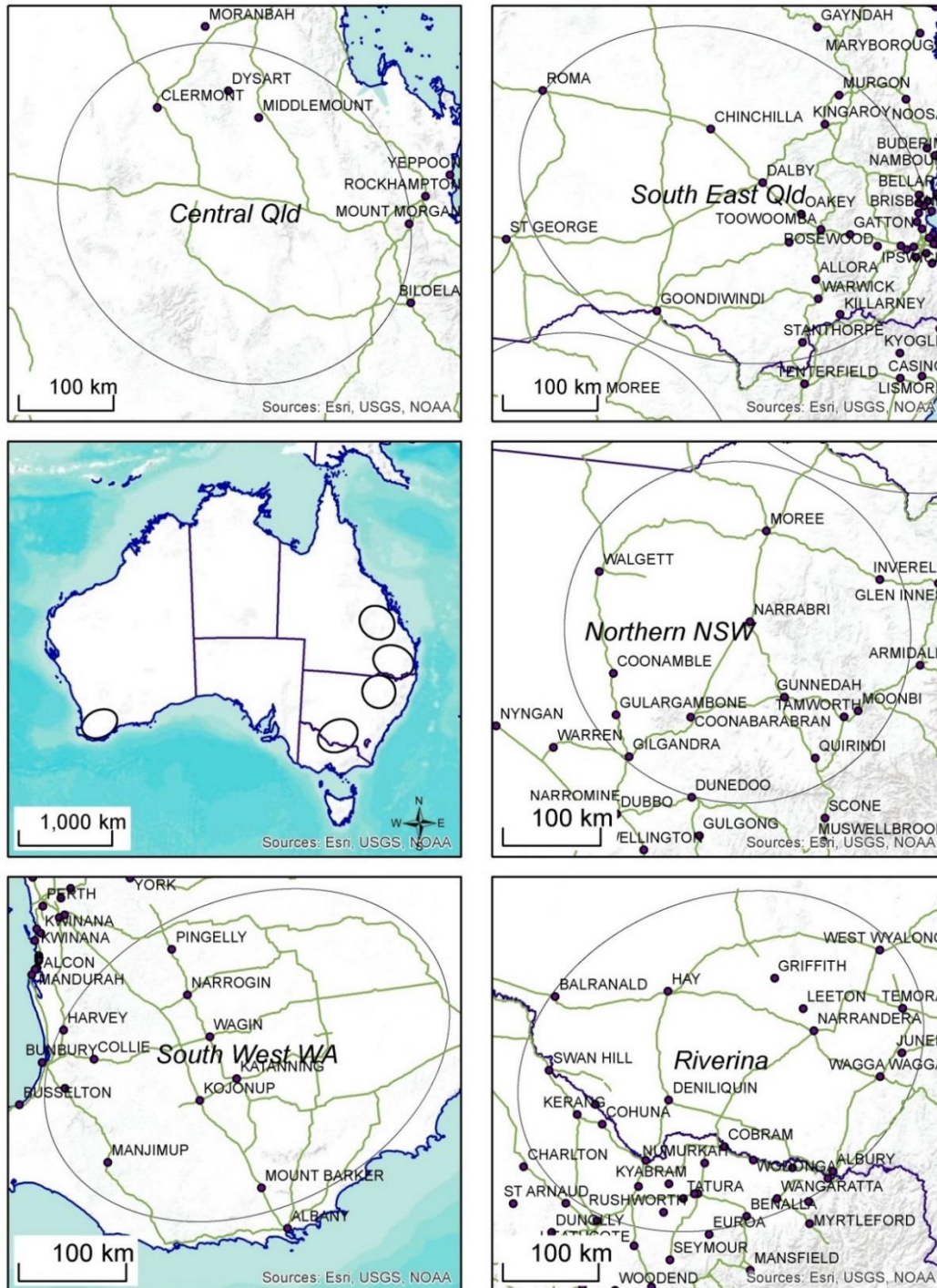


Figure 1. Location and localities shown for the five feedlot regions in which heat stress analyses have been carried out.

Table 4: Summary of the feedlot region sizes

<i>Region</i>	<i>Approx. Length (km)</i>	<i>Approx. width (km)</i>	<i>Area (km²)</i>
Central Qld	393	347	107178
South East Qld	445	347	121829
Northern NSW	358	353	99459
Riverina	440	339	117360
Southwest WA	397	289	90326

3.2 Historic analyses

3.2.1 Input datasets

To perform assessment of heat stress over these regions, several primary and derived daily gridded climate datasets were sourced from SILO which is an enhanced climate database operated by the Science Delivery Division of the Queensland Department of Science, Information Technology, Innovation and the Arts (DSITIA). Additionally, daily gridded 9 am and 3 pm vapour pressure data, with the same spatial resolution as the SILO data, were sourced from the Australian Bureau of Meteorology since the latter was not available as a SILO dataset.

The primary gridded datasets available were daily minimum and maximum temperature, vapour pressure, solar radiation and wind speed. However, to calculate HLI, and subsequently AHLU required deriving some additional variables from the base data. The prepared datasets are listed in Table 5, and descriptions of the processing undertaken are provided below.

3.2.2 Solar Irradiance

To derive HLI at the time of maximum daily temperature ($HLI_{t_{max}}$) utilising data for the maximum temperature (T_{max}) and 3 pm vapour pressure (VP15) it was necessary to generate an estimate of irradiance at 3 pm for each day. Daily gridded solar radiation datasets (MJ/m²/day) are available from BoM and SILO, but only the SILO data covered the historical date range required for this work, and is a blended dataset based on three sources: radiometer data, daily sunshine duration and cloud cover observations¹⁴. These data represent the daily total solar energy accumulated over a day, whereas to calculate the black globe temperature (BGT) required for the HLI, also needs an irradiance value (W/m²) to be calculated, which is an instantaneous value indicating the rate of solar radiation at a particular time of day.

The solar radiation function for extra-terrestrial radiation for hourly or shorter periods¹⁵ was applied for each 0.05° grid cell and day of the year to calculate both:

- estimated total daily extra-terrestrial radiation; and
- estimated extra-terrestrial radiation over a one hour period centred on 3pm.

The ratio of 3 pm radiation to total daily radiation was then applied to the gridded SILO radiation data to estimate the proportion of the total observed radiation occurring at 3 pm and thus an estimate of irradiance (W/m²) at that time. This method assumes that cloud cover and atmospheric conditions are constant throughout a day, however, since this approach makes use of observed data

¹⁴ Zajaczkowski, J., K. Wong & J. Carter (2013) Improved historical solar radiation gridded data for Australia. *Environmental Modelling & Software*, 49, 64-77.

¹⁵ Equation 28 in: Allen, R. G., L. S. Pereira, D. Raes & M. Smith. 1998. Crop evapotranspiration-Guidelines for computing crop water requirements-FAO Irrigation and drainage paper 56. In *FAO, Rome*, 6541.

it is an improvement on simpler methods which only estimate extra-terrestrial irradiance. Such methods do not account for cloud cover at all, and therefore overestimate solar radiation for cloudy days¹⁶.

Table 5: Description of the gridded climate datasets required for HLI calculations

Dataset	Abbreviation	Purpose	Source
Minimum and maximum daily temperature (°C)	T _{max} & T _{min}	Input into calculation of relative humidity and black globe temperature at time of T _{max} (RH _{tmax} , BGT _{tmax})	SILO ¹⁷
Vapour pressure at 9 am and 3 pm (hPa)	VP09 & VP15	Input into calculation of relative humidity at time of T _{min} and T _{max}	BoM ¹⁸
Solar radiation (MJ/m ² /day)	SRad	Used to derive 3pm irradiance in W/m ²	SILO ¹⁹
3 pm Irradiance (W/m ²)	Irrad	Input into BGT _{Tmax}	Estimated from SRad and ratio of extra-terrestrial radiation at 3pm
Wind speed (m/s)	WS	Input into HLI	CSIRO ²⁰ , however wind data were not available prior to 1975 so in-filled using daily averages
Relative humidity at T _{min} and T _{max} (%)	RH _{Tmin} & RH _{Tmax}	Input into HLI	Calculated from BoM VP09 and VP15 datasets and SILO T _{min} and T _{max}

3.2.3 Black globe temperature

Black globe temperature (BGT) is not available as a daily gridded dataset from SILO or BoM so it was necessary to utilise a predicted BGT based on air temperature (T_{min} and T_{max}) and solar irradiance (SR, W/m²) as developed by Petrov et al. (2003)²¹ for unshaded feedlot pens:

$$\text{BGT} = (1.33 \times \text{Temp}) - (2.65 \times \sqrt{\text{Temp}}) + (3.21 \times \log_{10}(\text{Irrad} + 1)) + 3.5 \quad (\text{eq } 1)$$

For the calculation of BGT_{Tmax}, the T_{max} and 3 pm irradiance were used. For BGT_{Tmin} the T_{min} was used and solar irradiance was assumed to be zero to represent night-time conditions.

¹⁶ Katestone Environmental. 2011. FLOT.334 Cattle Heat Load Forecast Service for 2005/2006 Summer. 56. MLA, North Sydney, NSW

¹⁷ Jeffrey, S. J., J. O. Carter, K. B. Moodie & A. R. Beswick (2001) Using spatial interpolation to construct a comprehensive archive of Australian climate data. *Environmental Modelling & Software*, 16, 309-330.

¹⁸ Jones, D. A., W. Wang & R. Fawcett (2009) High-quality spatial climate data-sets for Australia. *Australian Meteorological and Oceanographic Journal*, 58, 233-248.

¹⁹ Zajaczkowski, J., K. Wong & J. Carter (2013) Improved historical solar radiation gridded data for Australia. *Environmental Modelling & Software*, 49, 64-77.

²⁰ McVicar, T. R., T. G. Van Niel, L. T. Li, M. L. Roderick, D. P. Rayner, L. Ricciardulli & R. J. Donohue (2008) Wind speed climatology and trends for Australia, 1975-2006: Capturing the stilling phenomenon and comparison with near-surface reanalysis output. *Geophysical Research Letters*, 35, L20403.

²¹ Petrov, R., S. Lott, P. Binns, R. Cork & C. MacFarlane. 2003. FLOT.317. Measuring the microclimate of eastern Australian feedlots. MLA, North Sydney, NSW

3.2.4 Relative humidity

RH_{Tmin} and RH_{Tmax} datasets which are calculated from air temperature and relative humidity data are available from SILO. However, the RH_{Tmax} values are calculated from the 9 am rather than the 3 pm vapour pressure (VP) reading. For consistency, we have recalculated both the RH_{Tmin} and RH_{Tmax} datasets as described in Nidumolu et al. (2014)²². To summarise here, saturated vapour pressure (Es) was calculated using the equation

$$Es = 6.112 * \exp ((17.67 * \text{Temp}) / (\text{Temp} + 243.5)) \quad (\text{eq 2})$$

then relative humidity (RH) was calculated from the vapour pressure dataset (VP) and Es:

$$RH = (VP / Es) * 100 \quad (\text{eq 3})$$

Using this approach, relative humidity datasets were derived for 9 am using T_{min}, using VP09, and for 3 pm using T_{max} and VP15. This approach assumes that VP09 corresponds to that at the time of minimum temperature, and VP15 corresponds to the VP at the time of maximum temperature.

3.2.5 Wind speed

Obtaining gridded daily wind speed data for inclusion into the HLI calculation presented challenges. McVicar et al. (2008)²³ developed a gridded national daily wind speed dataset using spatial interpolation methods, based on BoM low-set anemometer data (2 m above ground). However, due to lack of quality historical station data, this dataset commences with 1975 and so does not cover the historical data range between 1963 and 1975, required for this study. In order to utilise the McVicar wind dataset for the missing years, average wind speed for each grid cell and each day of the year was calculated from the available data (1975 to 2012). Then those calculated average values used as the wind data for years 1963 to 1974. This approach clearly has some limitations for utilisation with the HLI, since the temporal relationship between wind speeds and temperature is important, and is not be captured in this in-filled dataset. These in-filled years were therefore omitted from trend analyses described below.

3.2.6 Calculation of HLI

The HLI was calculated as per the Gaughan et al. (2008)²⁴ method, also using a BGT threshold of 25 °C to apply different calculations based on high or low BGT. i.e.

$$\begin{aligned} &\text{If BGT} < 25 \\ &\quad HLI_{\text{low}} = (1.3 \times \text{BGT}) + (0.28 \times \text{RH}) - \text{WS} + 10.66 \quad (\text{eq 4}) \end{aligned}$$

$$\begin{aligned} &\text{Else} \\ &\quad HLI_{\text{high}} = (1.55 \times \text{BGT}) + (0.38 \times \text{RH}) - (0.5 \times \text{WS}) + \exp(2.4 - \text{WS}) + 8.62 \quad (\text{eq 5}) \end{aligned}$$

²² Nidumolu, U., S. Crimp, D. Gobbett, A. Laing, M. Howden & S. Little (2014) Spatio-temporal modelling of heat stress and climate change implications for the Murray dairy region, Australia. *Int J Biometeorol*, 58, 1095-108.

²³ McVicar, T. R., T. G. Van Niel, L. T. Li, M. L. Roderick, D. P. Rayner, L. Ricciardulli & R. J. Donohue (2008) Wind speed climatology and trends for Australia, 1975-2006: Capturing the stilling phenomenon and comparison with near-surface reanalysis output. *Geophysical Research Letters*, 35, L20403.

²⁴ Gaughan, J. B., T. L. Mader, S. M. Holt & A. Lisle (2008) A new heat load index for feedlot cattle. *Journal of Animal Science*, 86, 226-234.

HLI_{low} and HLI_{high} were combined using the sigmoidal weighting approach developed by Katestone Environmental (2011)²⁵ which is a modification of the Gaughan method, and provides a smoother transition in HLI values across the BGT threshold value:

$$FRACTION_{high} = 1.0 / (1.0 + \exp(-(\text{BGT} - 25.0) / 2.25)) \quad (\text{eq 6})$$

$$HLI = (FRACTION_{high} * HLI_{high}) + ((1 - FRACTION_{high}) * HLI_{low}) \quad (\text{eq 7})$$

This approach was used to calculate a daily $HLI_{T_{min}}$ (using T_{min} , $BGT_{T_{min}}$, $RH_{T_{min}}$ and WS) and also a daily $HLI_{T_{max}}$ (using T_{max} , $BGT_{T_{max}}$, $RH_{T_{max}}$ and WS). Note that wind speed data are only available as a single daily value, so the assumption has been made that wind speed is consistent across a whole 24 hour period. This is a recognised limitation since daily cycles in wind speed do occur. However daily cycles vary geographically, such as in relation to distance from the coast²⁶, and this limitation could only be addressed if more frequent wind data were available.

3.2.7 Calculation of AHLU

The excess heat load is calculated for $HLI_{T_{max}}$ and $HLI_{T_{min}}$ each day using

$$\begin{aligned} &\text{if } HLI > UL \\ &\quad \text{Excess} = HLI - UL \end{aligned} \quad (\text{eq 8})$$

$$\begin{aligned} &\text{Else if } HLI < LL \\ &\quad \text{Excess} = HLI - LL \end{aligned} \quad (\text{eq 9})$$

$$\begin{aligned} &\text{Else} \\ &\quad \text{Excess} = 0 \end{aligned}$$

with a fixed lower threshold (LL) of 77, and two representative upper thresholds (UL) as used by Gaughan et al. (2008). A HLI upper threshold of 86 was derived for unshaded Angus steers, and with minimal heat stress management in place, and an upper threshold of 96 for purebred *B. indicus*. The upper threshold of 96 could also be representative of less tolerant cattle, but where heat stress management strategies are in place. These thresholds were derived in consultation with MLA.

Gaughan et al. (2008)²⁷ provided a calculation for cattle heat load accumulation (AHLU) such that when HLI is above an upper threshold, heat load is accumulated, and when HLI is below a lower threshold, accumulated heat load is reduced. However Katestone Environmental (2013) use a revised form of this calculation in which heat load is lost at only half the rate at which it is gained. The rate of loss of heat load is the subject of current MLA funded research, however, in consultation with Katestone and MLA the latter approach is used here.

The AHLU was originally developed using a HLI calculated each 10 minutes. However the available weather data limits us to two calculated HLI values per day, one corresponding to T_{min} (assumed to be in the early morning) and the other corresponding to T_{max} (assumed to be mid-late afternoon).

²⁵ Katestone Environmental. 2011. FLOT.334 Cattle Heat Load Forecast Service for 2005/2006 Summer. 56. MLA, North Sydney, NSW

²⁶ Coppin, P. A., K. A. Ayotte & N. Steggel. 2003. Wind resource assessment in Australia - a planners guide. CSIRO: Wind Energy Research Unit, CSIRO Land and Water.

²⁷ Gaughan, J. B., T. L. Mader, S. M. Holt & A. Lisle (2008) A new heat load index for feedlot cattle. *Journal of Animal Science*, 86, 226-234.

The time interval between T_{\min} and T_{\max} is assumed to be 12 hours, and the AHLU calculations apply the $HLI_{T_{\max}}$ and $HLI_{T_{\min}}$ equally across each 12 hour interval. The AHLU is generated daily at the end of the day, i.e after the T_{\max} but before the T_{\min} as follows:

$$\begin{aligned} &\text{if Excess} > 0 \\ &\quad \text{New_AHLU} = \text{Old_AHLU} + \text{Excess} * T \end{aligned} \quad (\text{eq 10})$$

$$\begin{aligned} &\text{Else if Excess} < 0 \\ &\quad \text{New_AHLU} = \text{Old_AHLU} + \text{Excess} * T / 2.0 \end{aligned} \quad (\text{eq 11})$$

$$\begin{aligned} &\text{Else} \\ &\quad \text{New_AHLU} = \text{Old_AHLU} \end{aligned} \quad (\text{eq 12})$$

where T is the interval (in hours) between HLI estimates.

3.2.8 Summarising heat stress

Using the methods above, AHLU has been calculated on a daily basis from 1 Jan 1963 to the 31 Dec 2012, on the 0.05° grids covering each of the five main feedlot regions. The AHLU classes²⁸ shown in Table 1 were used to calculate summaries of the frequency (number of days the AHLU in or above each category per year, averaged over a decade), and duration (average length of continuous periods over the AHLU exceeds the class value per year, averaged over a decade).

3.3 Climate scenario analyses

3.3.1 Methods

Global circulation models (GCMs) are the main source of climate change projection information. These state-of-the art climate models provide credible simulations of climatic conditions at spatial scales of 2° of latitude and longitude (approximately 200 km²) and at large temporal scales such as monthly and longer timescales. However, they are considerably less reliable at finer spatial scales e.g. less than 200 km² and at shorter time scales e.g. seasonal to daily (particularly when it comes to simulating precipitation processes). Some effort has been made to assess the performance of these models in terms of their ability to simulate historical elements of the climate at a range of scales²⁹.

In the Smith and Chiew (2011)³⁰ internal report, produced as part of the South East Australian Climate Initiative (SEACI), the authors reviewed a range of peer-reviewed articles which assessed the skill of 22 commonly used GCMs in simulating certain key elements of global, national and regional climates.

The results suggest that only six of the 22 models have an adequate capability to simulate the El Niño Southern Oscillation (ENSO) and only four of the eleven models used to produce Murray Darling Basin annual rainfall are able to achieve this successfully. At a global scale 11 of the 22 models were able to adequately resolve global average rainfall. When assessed at hemispheric

²⁸ Katestone Environmental. 2011. FLOT.334 Cattle Heat Load Forecast Service for 2005/2006 Summer. 56. MLA, North Sydney, NSW

²⁹ Ramirez-Villegas, J., A. J. Challinor, P. K. Thornton & A. Jarvis (2013) Implications of regional improvement in global climate models for agricultural impact research. *Environmental Research Letters*, 8, 024018.

³⁰ Smith, I. N. & F. Chiew. 2011. Document and assess methods for generating inputs to hydrological models and extend delivery of projections across Victoria. Final report for SEACI Phase 3 Project 2.2.5P.

scales only half the models were able to simulate either Northern or Southern Hemispheric rainfall patterns successfully.

Table 6: A ranked list of 22 General circulation model simulations based on a weighted failure metric (after Smith and Chiew 2011).

GCM Name	Weighted failure rate
HADCM 3	0
MIROC 3.2 (High resolution)	8
GFDL 2.1	13
GFDL 2.0	20
MIROC 3.2 (medium resolution)	25
ECHO-G	33
HADGEM 1	33
ECHAM 5	38
MRI-CGCM 2.3.2	40
CCSM 3	44
CGCM 3.1	50
GISS-AOM	58
INM-CM 3.0	59
CGCM 3.2	63
FGOALS-G 1.0	63
CSIRO Mk 3.0	73
CNRM-CM 3	75
IPSL-CM 4	75
BCCR-BCM 2.0	88
GISS-ER	88
PCM	89
GISS-EH	100

While this method of assessment is somewhat subjective, it is apparent that some models consistently underperform. In particular, models with a failure rate greater than 65% were deemed of little or no use in the development of future projections (Table 6). On the other hand, some models consistently perform well and, while there is no agreed method for defining the “best” models, it is suggested that the top eight models listed in Table 6 are more likely to produce credible projections. In particular, these eight include the six models which have credible representations of ENSO – an important component of Australia’s climate variability. The bottom four models in the above list should not be used, and the top eight preferred. The middle ten may still be used, but with the knowledge that results from these are likely to be less reliable.

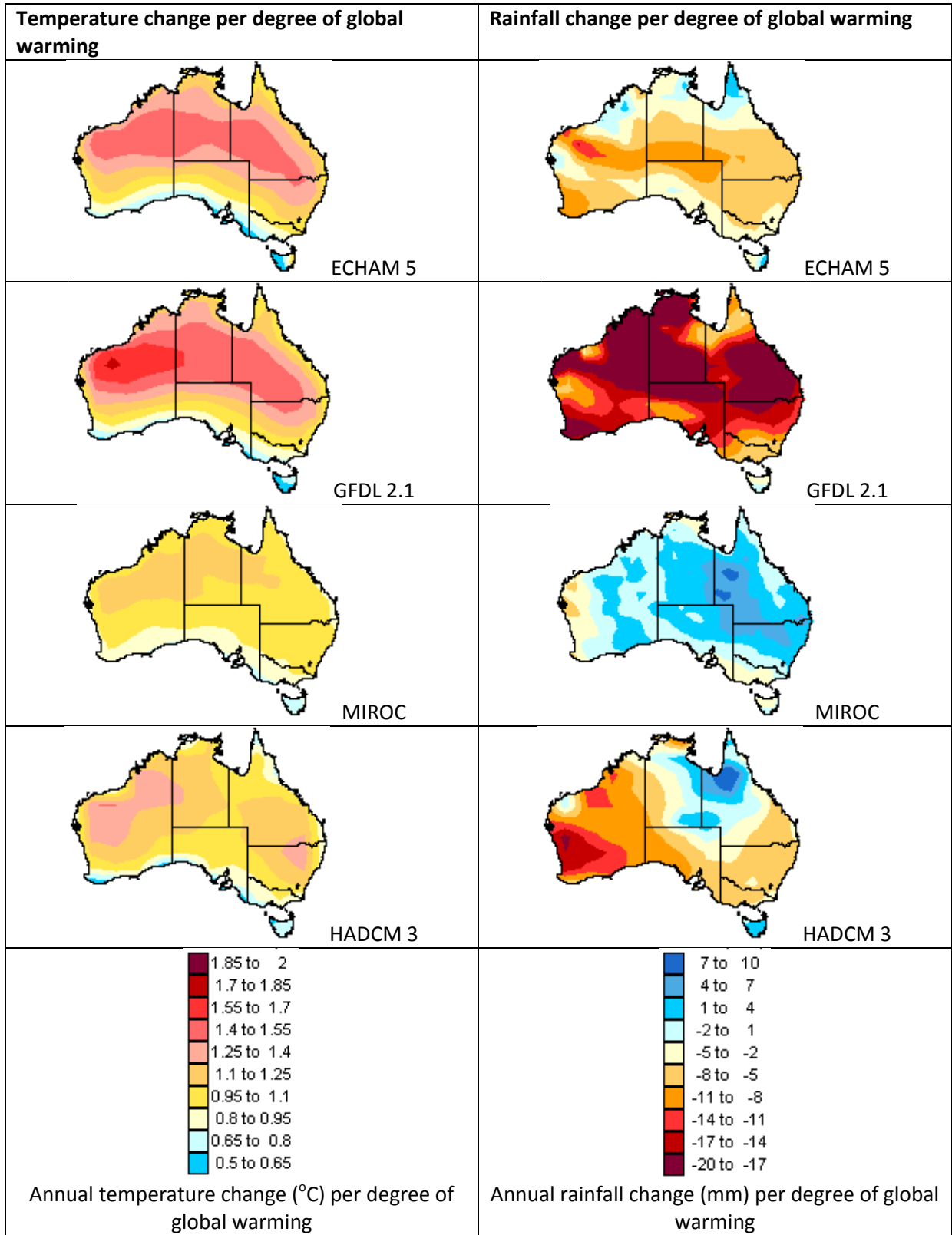


Figure 2: Patterns of annual temperature and annual rainfall change per degree of global warming for the four GCMs used in this study³¹.

³¹ CSIRO. 2014. OzClim Climate Change Scenario Generator. CSIRO.

For the purposes of this project we selected a sub-sample of top performing models as well as sample across the range of plausible future rainfall and temperature outcomes. We selected four models from the top eight that provided a range of possible future rainfall and temperature conditions. The GCMs used in this assessment are:

- HADCM 3 - from the Hadley Centre (HadCM3)
- MPI ECHAM 5 – from the Max Planck Institute for Meteorology
- MIROC3.2 - from the Centre for Climate System Research, University of Tokyo
- GFDL 2.1 - from the US Geophysical Fluid Dynamics Laboratory.

Figure 2 provides a visualisation of the patterns of temperature and rainfall change per degree of global warming for these models. The patterns include moderate to significant warming as well as drier and wetter future conditions.

The outputs of these models are generated at spatial scales of 2° of latitude and longitude (approximately 200 km²), and have been downscaled using the CSIRO conformal cubic atmospheric model (C-CAM)³² to a resolution of 0.5° of latitude and longitude (approximately 55 km grid). Six hourly maximum, minimum temperature; wind speed, relative humidity and solar radiation values were extracted from each model (Table 7) for a base period 1975 to 2012 and two twenty year periods centred on 2030 (2020 to 2040) and 2050 (2040 to 2060) respectively.

Table 7: Climate variables derived from the GCMs

<i>Variable (Name)</i>	<i>GCM data available</i>	<i>Periods analysed</i>
Minimum and maximum temperature (°C)	Daily min and max values	Baseline: 1975 - 2012 For 2030: 2020 - 2040 For 2050: 2040 - 2060
Irradiance (W/m ²)	Afternoon	
Wind speed (m/s)	Early morning & afternoon	
Relative humidity at Tmin and Tmax (%)	Daily min and max values	

3.3.2 Black globe temperature

Black globe temperature (BGT) was once again predicted using air temperature (Temp °C) and solar irradiance (W/m²) using the approach developed by Petrov (2007)³³ for unshaded feedlot pens. For the calculation of BGT_{Tmax}, the T_{max} and afternoon irradiance values were used. For BGT_{Tmin} the T_{min} was used and solar irradiance was assumed to be zero to represent night-time conditions.

3.3.3 Relative humidity

RH_{Tmin} and RH_{Tmax} data were sourced from the GCM outputs of daily minimum and maximum relative humidity respectively.

3.3.4 Wind speed

Gridded six hourly wind speed data were available from the GCMs for morning and afternoon, so no interpolation was required.

³² McGregor, J. L. 2005. C-CAM geometric aspects and dynamical formulation. In *CSIRO Atmospheric Research Technical Paper 70*, 43pp. Aspendale, Vic.: CSIRO Atmospheric Research.

³³ Petrov, R. 2007. The microclimate of Australian cattle feedlots. In *Faculty of Engineering and Surveying*. University of Southern Queensland.

3.3.5 Calculation of HLI and AHLU

The HLI index and daily AHLU were calculated as per the historical analysis (above).

The historical heat stress values calculated from the GCM data are not necessarily representative of observed conditions experienced over the same historical period, so it is not appropriate to compare the observed historical values (1975 – 2012) against the GCM 2030 and 2050 values. Instead, HLI and AHLU were calculated on a daily basis using the methods above, for a baseline period 1975 to 2012 and two twenty year periods centred on 2030 (2020 to 2040) and 2050 (2040 to 2060) using only the GCM data.

The change in heat stress frequency and duration for the 2030 and 2050 scenarios were compared against the GCM baseline period for each for each feedlot region. The calculated change between the GCM baseline and future projections was then used as a scaling factor and applied to the heat stress values calculated using historical data. In other words the proportional change in heat stress derived from the GCM data were applied to the historical observations. This was undertaken in order to develop a more representative change in future heat stress with the GCM scenarios.

As for the historical analysis, the AHLU classes shown in Table 1 were used to calculate summaries of the frequency (number of days the AHLU exceeds the class value per year, averaged over entire period), and duration (average length of continuous periods over the AHLU exceeds the class value per year, averaged over the entire period).

4 Results

4.1 Historical analysis

AHLU was summarised across each of the five regions, and for both the HLI upper thresholds for highly sensitive cattle (HLI threshold of 86) and less sensitive cattle (HLI threshold of 96). Regional summary statistics are presented in Appendix 1, showing the number of days per year for highly sensitive cattle (Table 8) and less sensitive cattle (Table 9), and mean duration of heat stress periods for highly sensitive cattle (Table 10) and less sensitive cattle (Table 11). These tables also summarise the annual trends from 1975 to 2012.

For each of the five feedlot regions, maps (Figure 5 through Figure 24, Appendix 3) show the mean number of heat stress days per year, and average duration of heat stress periods, in each of 4 AHLU classes. These maps also include the trend across all years from 1975 to 2012 (with the earlier years excluded due to inadequate wind data used in the HLI calculations prior to 1975)..

This analysis shows that:

1. Across the five regions, central Queensland experiences the highest level of heat stress (37 days per year for HLI 86 cattle). Heat stress is more prevalent in the north east of the central Queensland region than in the south west.
2. Southeast Queensland also experiences relatively high levels of heat stress (16.9 days per year for HLI 86 cattle), particularly in the north east, and lowest in the eastern central region.
3. Northern NSW experiences a moderate level of heat stress (14.5 days per year for HLI 86 cattle) which is highest in the north west of the region, and lowest in the east.
4. Riverina heat stress levels are relatively lower than other regions (9.3 days per year for HLI 86 cattle), with higher levels in the north of the region.

5. Southwest WA shows the lowest levels of HLI for the five regions (4.2 days per year for HLI 86 cattle), with the lowest levels in the coastal western region.
6. Heat stress frequency exhibits the strongest increasing trend in central Queensland, especially in the northwest of the region.
7. Much of northern NSW and western areas of the Riverina also show increasing trends.
8. Coastal areas of southeast Queensland and western areas of southwest WA show a decreasing trend in number of days and duration.
9. Average trends across all regions are for increasing number of days and duration of heat stress in 4 categories, for all regions except southeast Queensland which shows a slight decrease in heat stress in the lower categories (AHLU >1 and >20).

These findings apply for cattle, although for the less sensitive cattle, the patterns within regions of number of days and duration of heat stress periods are similar, but both the number of days and durations are substantially lower.

Figure 3 shows the regional averages of days and duration of heat stress periods using AHLU > 50 for the highly sensitive cattle (HLI threshold = 86) (Figure 3a), and for less sensitive cattle (HLI threshold = 96) (Figure 3c), and the mean length of heat stress periods in days for highly sensitive (Figure 3b), and less sensitive cattle respectively (Figure 3d).

When comparing decades (as in Figure 3) the highest number of days per year in most regions have been in the decades 1993-2002 and/or 2003-2012. In particular, for HLI96, the number of days with AHLU > 50 in the decade 2003-2012 in several regions (apart from CQ) was approximately double that of earlier decades.

Similarly the mean duration of heat stress periods with AHLU > 50 has been markedly higher in the same period for all regions except for central Queensland.

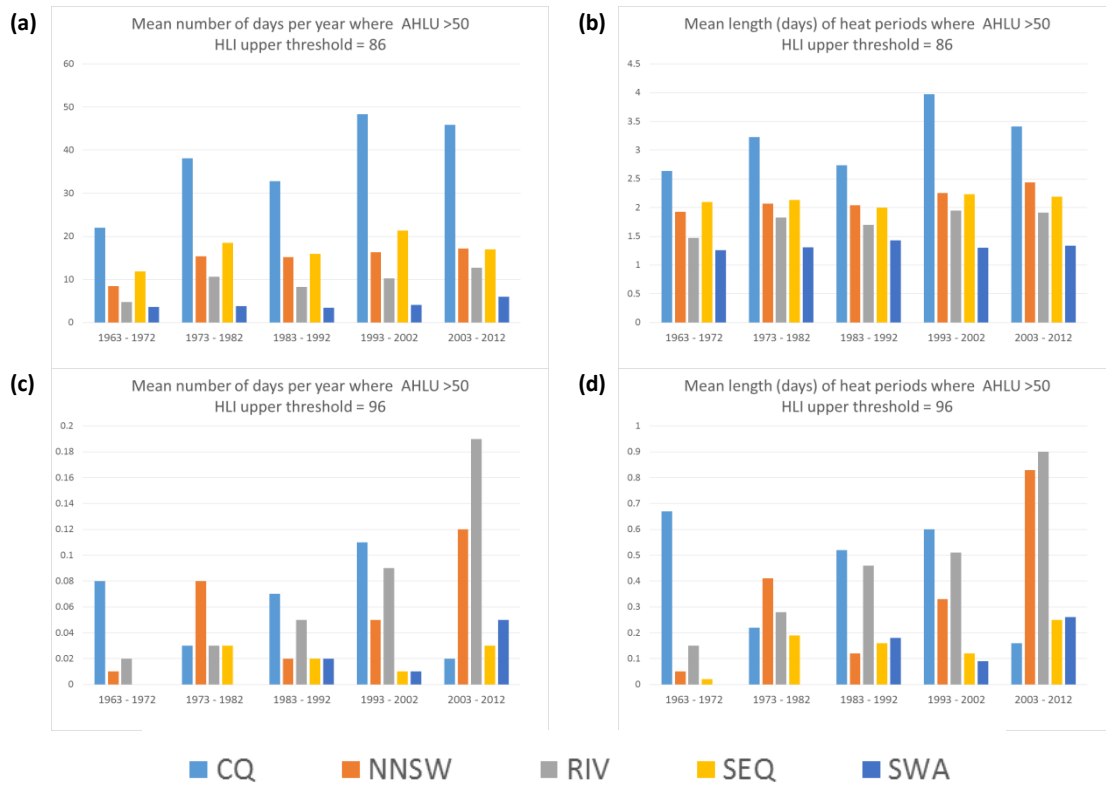


Figure 3. Decadal summaries of days with AHLU >50. For a HLI upper threshold of 86, (a) mean number of days per year (b) mean length of consecutive days. For a HLI upper threshold of 96, (c) mean number of days per year (d) mean length of consecutive periods.

4.2 AHLU under future scenarios

The analysis of AHLU changes predicted by four GCMs for the future years vary considerably between the five feedlot regions. The percentage change in both mean number of heat stress days, and mean length of heat stress periods (consecutive days) are presented in Table 12 to Table 15 (Appendix 2), and maps of the five study regions, Figure 25 to Figure 64 (Appendix 4). These analyses show wide ranging levels of heat stress, and amounts of change under future scenarios between regions.

For example, summarising only the high risk HLI days (where AHLU exceeds 50 units) for the more susceptible class of cattle (HLI threshold of 86) for example, the largest increases in heat stress by 2030 occur in central Queensland with rises in the number of days per year of between 6% and 13% (i.e. an increase from a mean of 37 days to 40 to 42 days per year). By 2050 the increase is between 16% and 19% (i.e. a further 3 to 5 annual days).

In other regions changes in heat stress are more modest despite significant increases in spring and summer temperatures. As with the historical analysis of the five regions, southwest Western Australia is projected to experience the lowest levels of high heat stress days (for highly susceptible cattle) with a 7% to 10% increase in 2030 but a 15% to 19% increase by 2050. This equates to an additional 0.3 to 0.4 average annual heat stress days by 2030 and an additional 0.6 or 0.8 days by 2050. Whilst the Riverina region showed the greatest percentage increases in mean number of high risk and extreme risk heat stress days, the average number of such days per year are low compared to Queensland and NSW regions, with susceptible cattle in the Riverina experiencing on average 0.8 to 1.5 high risk days per year in 2030 to 1.6 to 2.2 days per year in 2050.

Cattle in the two heat stress sensitivity classes (ie. with low and high HLI thresholds) show large differences in levels of heat stress experienced. The mean number of high risk days annually for less susceptible cattle (HLI threshold of 96) showed mean increases across the five regions of between 11% and 33% for 2030. For 2050 an increase of between 22% and 47% was simulated. For more susceptible cattle (HLI threshold of 86), the increases in high risk days are somewhat lower, with average increases across the five feedlot regions ranging from 5% to 16% for 2030 and 15% to 24% for 2050, however the mean annual number of high risk days for this class of cattle in 2030 range from 13 days in parts of southwest WA, to 117 days in parts of central Queensland. In 2050 the number of days range from 14 days in parts of southwest WA to 154 days in parts of southeast Queensland.

Comparing between 2030 and 2050, the relative heat stress increases are somewhat similar across the different regions, although the extreme increases for Central Queensland for 2050 (discussed above) appear to be one exception to this, even when compared with the predictions for 2030. Overall, the GCM scenarios show marked increases in heat stress risk. However, the predicted changes in temperature, relative humidity, wind and solar irradiance interact in varied and sometimes surprising ways.

The ECHAM5 model tends to predict the least severe increases in heat stress, whilst the MIROC model the greatest. This is surprising since, of the four GCMs, the MIROC model has the lowest level of temperature increase. The MIROC model also results in the most severe predictions for Central Queensland by 2050, with extreme risk AHLU days increasing by 505% for highly susceptible cattle, and increasing by 100% for the less susceptible cattle.

For the same period, the UK HADCM model results in lower increases, being 110% for highly susceptible cattle, and 80% for the less susceptible cattle. However, for the lower risk SW WA region, these two models produce much more similar increases of 35% and 34% for low tolerance cattle, and 21% and 19% for low susceptibility cattle.

The maps of AHLU changes under future climate scenarios (Figure 25 to Figure 64 in Appendix 4) demonstrate the high degree of spatial variation within the five feedlot regions. The spatial variation in the HLI and AHLU predictions mean it is difficult to summarise consistent patterns to compare between the models, and each region needs to be examined on a case by case basis, especially when assessing the range of changes within each region, and illustrated by the maps.

5 Discussion and conclusions

The aim of this study was to examine patterns and trends of heat stress at regional scales using the HLI and AHLU. Being undertaken at a regional scale, these analyses do not take into account factors at the scale of individual feedlots which impact the heat loads and heat stress experienced by cattle. Meteorological parameters which play a role in heat stress, such as temperature, humidity wind speed and solar radiation can be influenced at a local scale by many environmental and local factors including nearby vegetation cover, presence of water bodies, elevation, slope and landform. In addition attributes of the cattle, such as genotype and coat colour will influence their susceptibility to heat stress, and management actions such as provision of shade, wet manure removal are also shown to influence cattle sensitivity to heat stress.

These results have compared heat stress using two different cattle heat stress sensitivity levels. These represent inherent sensitivity resulting from cattle genotype, as well as indicate the benefits that may result from implementing heat stress management practices (HLI upper threshold of 96).

(Gaughan et al. 2008)³⁴ indicated that cattle of *Bos indicus* genotype may have a HLI upper threshold of around 10 units higher than British *Bos taurus* cattle. Unsurprisingly these results show substantially lower numbers of days per year, and duration of heat stress periods for the less sensitive class. This highlights the potential benefit of cattle genotype selection as one of the management actions that reduce sensitivity to heat stress. However, the future climate scenario analyses also indicate that the percentage increases in heat stress days will be relatively higher for the less susceptible class (HLI threshold of 96), than for the more susceptible class (HLI threshold of 86).

At individual feedlot sites, climatic data can be monitored at a fine temporal scale (e.g. data recorded every few minutes). However, scaling up to a regional scale is not possible. In addition this local data tends to be collected over discrete periods, too short for meaningful trend analyses to be performed. Since the influence of HLI on cattle and its aggregation into the AHLU is time dependent, the calculated values from this approach are likely to differ from values calculated using local station data at higher temporal resolution. For this reason heat loads experienced at any one location are unlikely to correspond exactly to those shown by this analysis, and these results therefore need to be interpreted with the scale of the input data in mind, and not translated quantitatively to a local feedlot scale. By omitting the local factors highlighted above, these regionalised results are able to demonstrate patterns and trends in heat stress that would not be readily summarised otherwise.

Wind data: Due to the unavailability of high quality gridded wind speed datasets for the period prior to 1975 we generated an in-filled wind dataset of daily wind speeds from the available years of data. The sensitivity of the HLI to wind speed is expected to be low, but it would be of value to develop an alternative gridded wind speed dataset. A statistical modelling approach such as using the spTimer (Bakar and Sahu 2013)³⁵ software package for the R statistical environment (R Development Core Team 2011)³⁶ may be an way to do this.

AHLU Spikes: Time-series of daily AHLU values calculated in the manner described in this report show periods of substantial spikes where AHLU can exceed 1000. This appears somewhat problematic, especially when an AHLU > 100. It appears that due to low rates of heat load loss, these periods can extend over several days or weeks. Figure 4 illustrates one such period in the Central Queensland region during early 1998.

Just as the AHLU should not fall below zero, since zero represents an animal in thermal equilibrium, it might also be appropriate to modify the AHLU calculation to impose an upper limit on AHLU. This problem is recognised by Katestone Environmental and has been identified by Brown-Brandl (2013)³⁷ and may require an improved understanding of animal physiological responses to heat stress. This relates to a point also made by Hahn et al. (2009)³⁸ that while thermal indices may be refined and improved, it is in understanding how the indices translate to biological responses that is most likely

³⁴ Gaughan, J. B., T. L. Mader, S. M. Holt & A. Lisle (2008) A new heat load index for feedlot cattle. *Journal of Animal Science*, 86, 226-234.

³⁵ Bakar, K. S. & S. K. Sahu. 2013. spTimer: Spatio-Temporal Bayesian Modelling Using R. Version 0.9-1. URL: <http://cran.r-project.org/web/packages/spTimer/index.html> CRAN publication.

³⁶ R: A language and environment for statistical computing. R Foundation for Statistical Computing, Vienna, Austria.

³⁷ Brown-Brandl, T. 2013. Managing thermal stress in feedlot cattle: environment, animal susceptibility and management options from an US perspective. In *Livestock housing: Modern management to ensure optimal health and welfare of farm animals*, eds. A. Aland & T. Banhazi, 1-491. Wageningen Academic Publishers.

³⁸ Hahn, G. L., J. B. Gaughan, T. L. Mader & R. A. Eigenberg. 2009. Chapter 5: Thermal indices and their applications for livestock environments. In *Livestock Energetics and Thermal Environmental Management*, ed. J. A. DeShazer, 113-130. St Joseph, Mich.: American Society of Agricultural and Biological Engineers.

to assist in tactical decision making to assist in managing livestock exposed to periods of climatic heat stress.

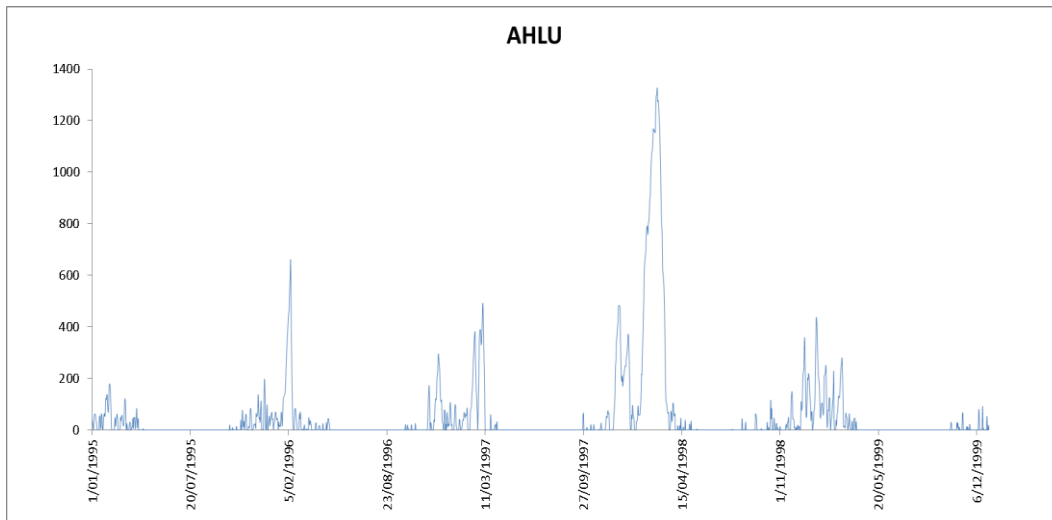


Figure 4. Time series of AHLU for a single point in the Central Queensland region. AHLU data are shown for 1995 to 1999 inclusive.

6 Bibliography

- Allen, R. G., L. S. Pereira, D. Raes & M. Smith. 1998. Crop evapotranspiration-Guidelines for computing crop water requirements-FAO Irrigation and drainage paper 56. In *FAO, Rome*, 6541.
- Bakar, K. S. & S. K. Sahu. 2013. spTimer: Spatio-Temporal Bayesian Modelling Using R. Version 0.9-1. URL: <http://cran.r-project.org/web/packages/spTimer/index.html> CRAN publication.
- Brown-Brandl, T. 2013. Managing thermal stress in feedlot cattle: environment, animal susceptibility and management options from an US perspective. In *Livestock housing: Modern management to ensure optimal health and welfare of farm animals*, eds. A. Aland & T. Banhazi, 1-491. Wageningen Academic Publishers.
- Coppin, P. A., K. A. Ayotte & N. Steggel. 2003. Wind resource assessment in Australia - a planners guide. CSIRO: Wind Energy Research Unit, CSIRO Land and Water.
- CSIRO. 2014. OzClim Climate Change Scenario Generator. CSIRO.
- Gaughan, J., N. Lacetera, S. E. Valtorta, H. H. Khalifa, L. Hahn & T. Mader. 2009. Response of domestic animals to climate challenges. In *Biometeorology for adaptation to climate variability and change*, 131-170. Springer.
- Gaughan, J. B., T. L. Mader, S. M. Holt & A. Lisle (2008) A new heat load index for feedlot cattle. *Journal of Animal Science*, 86, 226-234.
- Hahn, G. L., J. B. Gaughan, T. L. Mader & R. A. Eigenberg. 2009. Chapter 5: Thermal indices and their applications for livestock environments. In *Livestock Energetics and Thermal Environmental Management*, ed. J. A. DeShazer, 113-130. St Joseph, Mich.: American Society of Agricultural and Biological Engineers.
- Jeffrey, S. J., J. O. Carter, K. B. Moodie & A. R. Beswick (2001) Using spatial interpolation to construct a comprehensive archive of Australian climate data. *Environmental Modelling & Software*, 16, 309-330.
- Jones, D. A., W. Wang & R. Fawcett (2009) High-quality spatial climate data-sets for Australia. *Australian Meteorological and Oceanographic Journal*, 58, 233-248.
- Katestone Environmental. 2011. FLOT.334 Cattle Heat Load Forecast Service for 2005/2006 Summer. 56. MLA, North Sydney, NSW
- . 2013. Accumulated Heat Load Units (AHLU).
- Kennedy, P. & P. Cronjé. 2005. FLOT.314 - Dietary strategies for amelioration of heat load in feedlot cattle Meat & Livestock Australia Limited.
- McGregor, J. L. 2005. C-CAM geometric aspects and dynamical formulation. In *CSIRO Atmospheric Research Technical Paper 70*, 43pp. Aspendale, Vic.: CSIRO Atmospheric Research.
- McVicar, T. R., T. G. Van Niel, L. T. Li, M. L. Roderick, D. P. Rayner, L. Ricciardulli & R. J. Donohue (2008) Wind speed climatology and trends for Australia, 1975-2006: Capturing the stilling phenomenon and comparison with near-surface reanalysis output. *Geophysical Research Letters*, 35, L20403.
- Meat and Livestock Australia. 2006. Tips and tools: Heat load in feedlot cattle. North Sydney: Meat and Livestock Australia.
- Nidumolu, U., S. Crimp, D. Gobbett, A. Laing, M. Howden & S. Little (2014) Spatio-temporal modelling of heat stress and climate change implications for the Murray dairy region, Australia. *Int J Biometeorol*, 58, 1095-108.
- Nidumolu, U. B., S. Crimp, D. Gobbett, A. Laing & S. Little (2010) Heat stress in dairy cattle in northern Victoria: responses to a changing climate. *CSIRO Climate Adaptation Flagship Working Paper No. 10*. <http://www.csiro.au/Organisation-Structure/Flagships/Climate-Adaptation-Flagship/CAF-working-papers/CAF-working-paper-10.aspx> (last accessed 19th Nov 2014).

- Petrov, R. 2007. The microclimate of Australian cattle feedlots. In *Faculty of Engineering and Surveying*. University of Southern Queensland.
- Petrov, R., S. Lott, P. Binns, R. Cork & C. MacFarlane. 2003. FLOT.317. Measuring the microclimate of eastern Australian feedlots. MLA, North Sydney, NSW
- R: A language and environment for statistical computing. R Foundation for Statistical Computing, Vienna, Austria.
- Ramirez-Villegas, J., A. J. Challinor, P. K. Thornton & A. Jarvis (2013) Implications of regional improvement in global climate models for agricultural impact research. *Environmental Research Letters*, 8, 024018.
- Sackett, D., P. Holmes, K. Abbott, S. Jephcott & M. Barber. 2006. Assessing the economic cost of endemic disease on the profitability of Australian beef cattle and sheep producers. AHW.087. North Sydney NSW.
- Smith, I. N. & F. Chiew. 2011. Document and assess methods for generating inputs to hydrological models and extend delivery of projections across Victoria. Final report for SEACI Phase 3 Project 2.2.5P.
- Zajackowski, J., K. Wong & J. Carter (2013) Improved historical solar radiation gridded data for Australia. *Environmental Modelling & Software*, 49, 64-77.

7 Acknowledgements

The project was made possible by funding from CSIRO's Agriculture Flagship and MLA. Mick Hartcher (CSIRO) assisted with SILO datasets. Frank Quintarelli (Katestone Environmental Pty Ltd) provided helpful advice regarding AHLU calculations. Uday Nidumolu provided helpful comments on a draft version of this report.

Appendix 1 – Summaries of historical heat stress

Table 8. Summaries for the five study regions, of the mean number of days per year in each of four heat stress categories, with a HLI upper threshold of 86. Trends shown apply to the period 1975 to 2012

Region	AHLU Range	Mean number of days/year			Trend in days/year		
		Min	Max	Mean	Min	Max	Mean
CQ	>1	5.3	156.9	93.0	-0.47	1.14	0.50
	>20	2.3	129.3	68.4	-0.48	1.09	0.51
	>50	0.3	94.1	37.4	-0.43	1.07	0.49
	>100	0.0	63.2	15.2	-0.30	0.89	0.32
SEQ	>1	4.5	103.1	55.5	-0.97	0.72	-0.10
	>20	1.9	77.6	37.2	-0.93	0.72	-0.04
	>50	0.2	44.3	16.9	-0.75	0.55	0.03
	>100	0.0	18.3	3.8	-0.38	0.30	0.02
NNSW	>1	0.7	77.2	43.9	-0.51	0.62	0.04
	>20	0.3	58.3	30.2	-0.32	0.54	0.07
	>50	0.0	32.6	14.5	-0.11	0.42	0.09
	>100	0.0	12.1	3.7	-0.01	0.15	0.05
RIV	>1	6.2	43.1	26.8	-0.24	0.65	0.10
	>20	3.3	31.8	18.4	-0.19	0.56	0.11
	>50	0.8	18.3	9.3	-0.10	0.37	0.10
	>100	0.1	6.0	2.3	0.00	0.24	0.07
SWA	>1	1.1	31.9	14.9	-0.03	0.92	0.19
	>20	0.4	22.6	9.5	-0.04	0.67	0.13
	>50	0.1	12.1	4.2	-0.04	0.40	0.07
	>100	0.0	3.0	0.7	-0.04	0.17	0.02

Table 9. Summaries for the five study regions, of the mean number of days per year in each of four heat stress categories, with a HLI upper threshold of 96. Trends shown apply to the period 1975 to 2012.

Region	AHLU Range	Mean number of days/year			Trend in days/year		
		Min	Max	Mean	Min	Max	Mean
CQ	>1	0.0	7.0	1.7	-0.05	0.15	0.03
	>20	0.0	3.1	0.5	-0.04	0.05	0.01
	>50	0.0	0.9	0.1	-0.02	0.01	0.00
	>100	0.0	0.3	0.0	-0.01	0.00	0.00
SEQ	>1	0.0	3.7	0.7	-0.09	0.05	0.00
	>20	0.0	1.6	0.2	-0.05	0.03	0.00
	>50	0.0	0.5	0.0	-0.01	0.02	0.00
	>100	0.0	0.1	0.0	0.00	0.01	0.00
NNSW	>1	0.0	3.6	1.0	-0.03	0.07	0.01
	>20	0.0	1.8	0.4	-0.02	0.04	0.01
	>50	0.0	0.5	0.1	0.00	0.02	0.00
	>100	0.0	0.1	0.0	0.00	0.00	0.00
RIV	>1	0.0	2.6	0.9	-0.01	0.13	0.03
	>20	0.0	1.3	0.4	-0.01	0.08	0.02
	>50	0.0	0.5	0.1	0.00	0.04	0.01
	>100	0.0	0.1	0.0	0.00	0.01	0.00
SWA	>1	0.0	1.3	0.2	-0.03	0.11	0.01
	>20	0.0	0.8	0.1	-0.01	0.08	0.01
	>50	0.1	0.3	0.0	0.00	0.03	0.00
	>100	0.0	0.1	0.0	0.00	0.01	0.00

Table 10: Summaries for the five study regions, of the mean duration of periods in each of four heat stress categories, with a HLI upper threshold of 86. Trends shown apply to the period 1975 to 2012.

Region	AHLU Range	Mean duration of heat stress periods			Trend in duration (days)		
		Min	Max	Mean	Min	Max	Mean
CQ	>1	1.7	7.8	4.9	-0.01	0.10	0.03
	>20	1.3	6.9	4.0	-0.02	0.09	0.03
	>50	0.8	6.6	3.2	-0.03	0.10	0.03
	>100	0.2	13.3	4.6	-0.24	0.38	0.07
SEQ	>1	1.5	4.6	3.2	-0.04	0.04	0.00
	>20	1.2	3.8	2.7	-0.03	0.04	0.01
	>50	0.9	3.3	2.1	-0.03	0.03	0.00
	>100	0.0	5.4	2.4	-0.07	0.05	0.00
NNSW	>1	1.2	4.1	3.0	-0.01	0.04	0.01
	>20	1.1	3.6	2.6	-0.01	0.04	0.02
	>50	0.2	3.0	2.1	0.00	0.04	0.02
	>100	0.0	4.2	2.2	0.00	0.07	0.03
RIV	>1	1.6	2.8	2.3	-0.01	0.03	0.01
	>20	1.4	2.6	2.0	-0.01	0.03	0.01
	>50	1.2	2.3	1.8	-0.01	0.05	0.01
	>100	0.3	2.8	1.8	-0.02	0.05	0.02
SWA	>1	1.1	2.2	1.6	-0.01	0.03	0.00
	>20	1.0	2.0	1.5	-0.02	0.02	0.00
	>50	0.6	1.9	1.3	-0.03	0.03	0.00
	>100	0.0	2.4	1.2	-0.04	0.04	0.00

Table 11. Summaries for the five study regions, of the mean duration of periods in each of four heat stress categories, with a HLI upper threshold of 96. Trends shown apply to the period 1975 to 2012.

Region	AHLU Range	Mean duration of heat stress periods			Trend in duration (days)		
		Min	Max	Mean	Min	Max	Mean
CQ	>1	0.0	2.4	1.3	-0.02	0.04	0.00
	>20	0.0	2.5	1.0	-0.03	0.03	0.00
	>50	0.0	3.1	0.4	-0.02	0.01	0.00
	>100	0.0	1.6	0.0	-0.01	0.00	0.00
SEQ	>1	0.0	2.8	1.2	-0.03	0.03	0.00
	>20	0.0	2.7	0.8	-0.03	0.02	0.00
	>50	0.0	2.4	0.1	-0.01	0.02	0.00
	>100	0.0	1.0	0.0	0.00	0.01	0.00
NNSW	>1	0.0	2.7	1.2	-0.01	0.04	0.01
	>20	0.0	2.5	0.9	-0.01	0.03	0.01
	>50	0.0	2.1	0.3	0.00	0.02	0.00
	>100	0.0	0.6	0.0	0.00	0.00	0.00
RIV	>1	0.0	2.3	1.3	-0.02	0.04	0.01
	>20	0.0	2.2	1.1	-0.01	0.04	0.01
	>50	0.0	1.5	0.5	0.00	0.02	0.00
	>100	0.0	0.4	0.1	0.00	0.01	0.00
SWA	>1	0.0	2.2	0.9	-0.02	0.04	0.00
	>20	0.0	1.7	0.5	-0.01	0.03	0.00
	>50	0.0	1.0	0.1	0.00	0.02	0.00
	>100	0.0	0.6	0.0	0.00	0.01	0.00

Appendix 2 – Summaries of future scenario heat stress

Table 12. Summaries for the five study regions, of the percentage difference in scenarios for 2030 and 2050 in mean number of days per year in each of four heat stress categories, with a HLI upper threshold of 86. Figures for 2030 and 2050 are the percentage difference from summaries of the period 1975 to 2012.

	AHLU level	2030				2050			
		ECHAM5	GFDLCM21	MIROC3	UKHADCM3	ECHAM5	GFDLCM21	MIROC3	UKHADCM3
Central Qld	Low risk	8	11	9	5	14	14	14	13
	Medium risk	9	12	10	5	16	16	16	14
	High risk	10	13	12	6	18	18	19	16
	Extreme risk	12	16	15	7	22	22	24	20
South East Qld	Low risk	9	12	10	6	17	17	19	16
	Medium risk	10	12	11	6	18	18	21	17
	High risk	11	14	13	7	20	21	24	20
	Extreme risk	16	20	18	9	28	28	33	28
Northern NSW	Low risk	7	10	9	4	13	15	16	13
	Medium risk	7	11	10	4	14	17	18	14
	High risk	9	13	13	5	17	19	21	17
	Extreme risk	14	18	19	8	25	26	30	25
Riverina	Low risk	4	11	9	6	13	15	16	16
	Medium risk	5	13	11	7	14	18	18	18
	High risk	7	16	15	9	17	22	24	23
	Extreme risk	11	23	24	14	24	32	37	35
Southwest WA	Low risk	6	9	8	7	12	14	11	14
	Medium risk	6	10	9	8	13	15	12	16
	High risk	7	10	10	10	15	17	15	19
	Extreme risk	9	13	15	15	20	25	23	29

Table 13. Summaries for the five study regions, of the percentage difference in mean number of days per year in scenarios for 2030 and 2050 in each of four heat stress categories, with a HLI upper threshold of 96. Figures for 2030 and 2050 are the percentage difference from summaries of the period 1975 to 2012.

	AHLU level	2030				2050			
		ECHAM5	GFDLCM21	MIROC3	UKHADCM3	ECHAM5	GFDLCM21	MIROC3	UKHADCM3
Central Qld	Low risk	9	11	11	6	17	17	20	18
	Medium risk	10	13	13	7	20	20	24	21
	High risk	14	17	18	11	27	25	31	29
	Extreme risk	29	33	34	21	52	45	56	50
South East Qld	Low risk	12	17	17	12	22	22	27	29
	Medium risk	14	24	18	13	28	27	33	36
	High risk	19	30	26	12	36	32	38	36
	Extreme risk	35	41	48	24	60	58	74	58
Northern NSW	Low risk	13	16	17	7	23	22	26	23
	Medium risk	17	19	21	9	28	27	32	27
	High risk	23	26	30	13	39	36	45	36
	Extreme risk	41	42	55	21	65	60	83	53
Riverina	Low risk	9	22	22	14	22	30	34	33
	Medium risk	11	24	26	15	24	33	38	37
	High risk	14	28	33	19	28	41	47	44
	Extreme risk	21	38	48	25	39	57	72	59
Southwest WA	Low risk	9	13	12	16	20	26	22	30
	Medium risk	10	13	14	17	22	29	27	32
	High risk	11	16	16	17	22	34	32	35
	Extreme risk	12	20	22	25	26	45	38	42

Table 14. Summaries for the five study regions, of the percentage difference in mean duration of periods in scenarios for 2030 and 2050 in each of four heat stress categories, with a HLI upper threshold of 86. Figures for 2030 and 2050 are the percentage difference from summaries of the period 1975 to 2012.

	AHLU level	2030				2050			
		ECHAM5	GFDLCM21	MIROC3	UKHADCM3	ECHAM5	GFDLCM21	MIROC3	UKHADCM3
Central Qld	Low risk	57	103	86	19	467	396	670	210
	Medium risk	53	97	80	17	466	302	636	169
	High risk	42	80	74	14	472	251	629	133
	Extreme risk	33	54	64	11	455	319	505	110
South East Qld	Low risk	14	19	22	5	28	31	37	36
	Medium risk	15	22	26	5	28	32	40	39
	High risk	18	26	32	8	32	36	46	45
	Extreme risk	24	34	40	12	47	39	61	58
Northern NSW	Low risk	9	15	26	0	22	21	33	34
	Medium risk	11	18	28	1	29	24	40	37
	High risk	14	24	33	5	38	31	52	44
	Extreme risk	28	39	47	17	50	45	74	65
Riverina	Low risk	1	16	21	11	19	24	33	30
	Medium risk	3	17	25	15	21	27	39	34
	High risk	5	22	33	20	23	32	49	43
	Extreme risk	12	28	52	24	28	41	66	58
Southwest WA	Low risk	5	7	12	15	18	13	17	29
	Medium risk	4	9	13	16	18	16	18	30
	High risk	5	11	16	17	18	21	23	31
	Extreme risk	7	12	21	19	21	30	35	34

Table 15. Summaries for the five study regions, of the percentage difference in mean duration of periods in scenarios for 2030 and 2050 each of four heat stress categories, with a HLI upper threshold of 96. Figures for 2030 and 2050 are the percentage difference from summaries of the period 1975 to 2012.

	AHLU level	2030				2050			
		ECHAM5	GFDLCM21	MIROC3	UKHADCM3	ECHAM5	GFDLCM21	MIROC3	UKHADCM3
Central Qld	Low risk	10	14	19	11	24	21	32	37
	Medium risk	15	20	26	16	35	29	40	44
	High risk	26	34	39	23	55	46	66	55
	Extreme risk	46	78	67	28	96	100	104	80
South East Qld	Low risk	13	14	21	9	26	20	35	36
	Medium risk	15	18	25	10	30	24	41	37
	High risk	18	25	32	10	33	31	49	39
	Extreme risk	25	34	39	16	45	50	69	48
Northern NSW	Low risk	16	20	26	7	26	26	41	33
	Medium risk	18	22	30	8	28	29	45	32
	High risk	21	25	34	10	30	35	51	33
	Extreme risk	30	26	39	12	40	45	65	37
Riverina	Low risk	5	12	27	13	13	17	31	29
	Medium risk	7	12	27	13	13	18	32	28
	High risk	8	13	29	13	13	21	36	26
	Extreme risk	12	13	32	14	17	22	47	26
Southwest WA	Low risk	4	7	10	14	13	20	20	20
	Medium risk	5	7	11	13	11	20	19	18
	High risk	4	6	12	13	8	18	18	17
	Extreme risk	1	8	16	14	6	14	21	19

Appendix 3 – Maps of historical heat stress

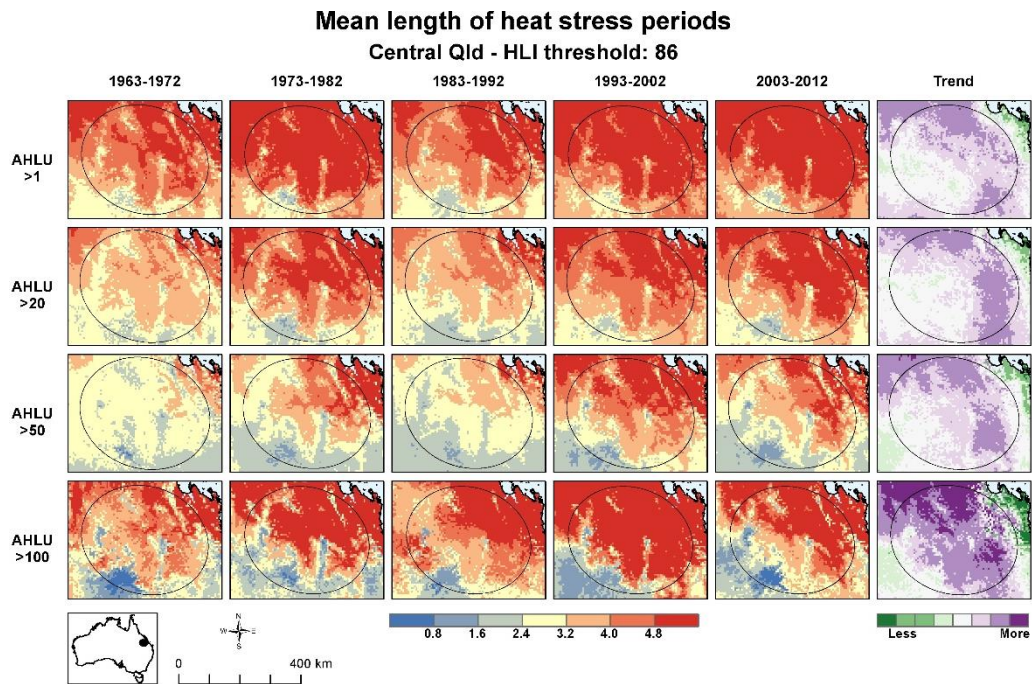


Figure 5. Decadal means of length of consecutive periods of heat stress for Central Queensland, and HLI upper limit of 86.

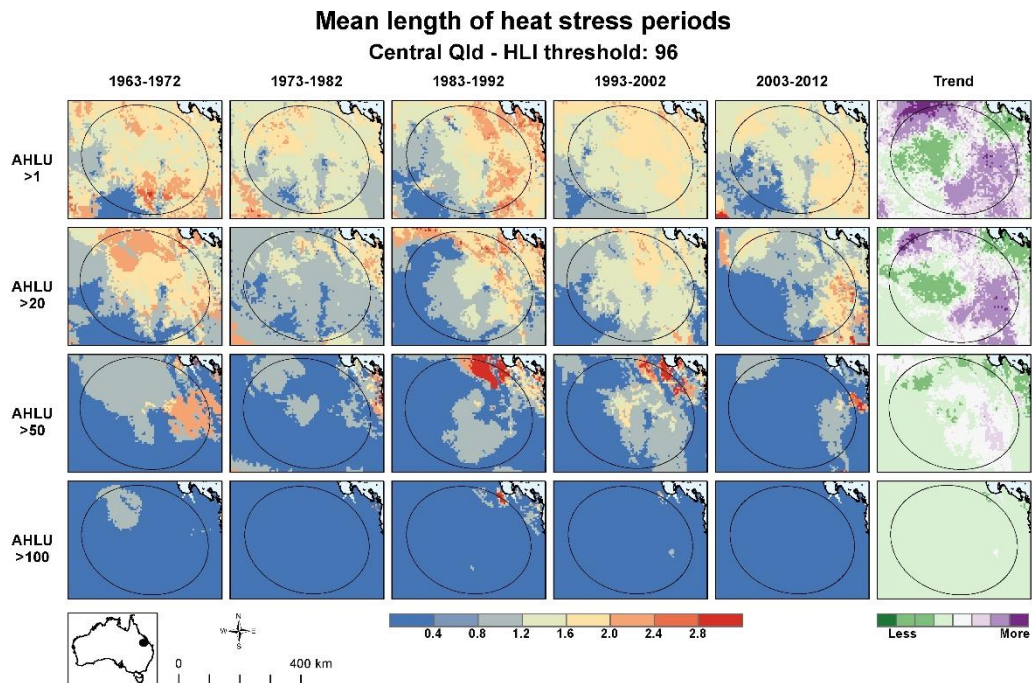


Figure 6. Decadal means of length of consecutive periods of heat stress for Central Queensland, and HLI upper limit of 96.

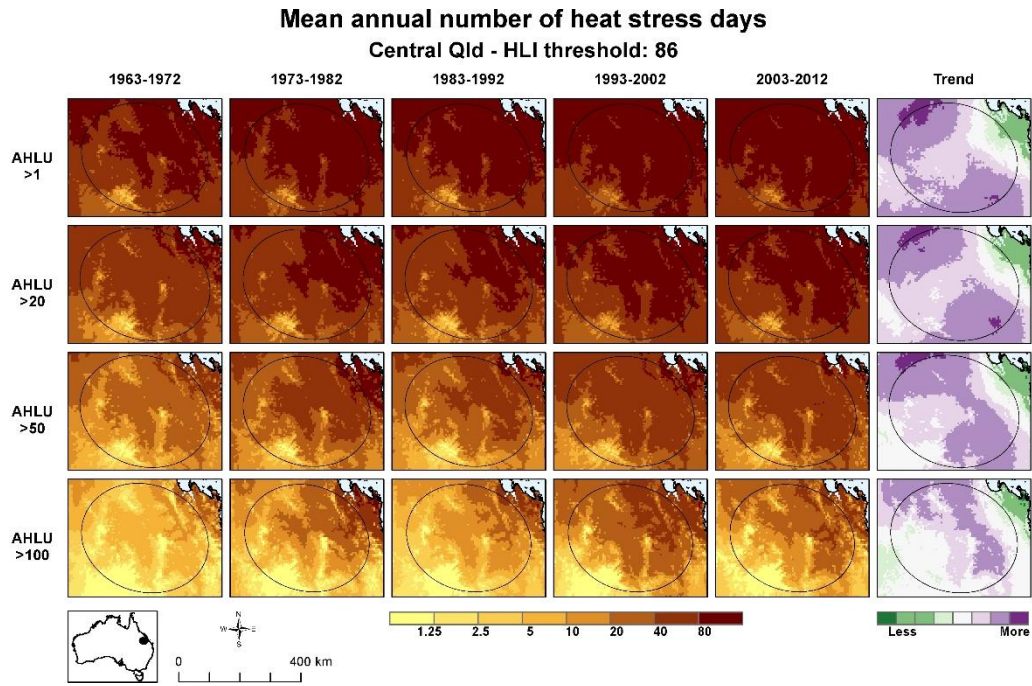


Figure 7. Decadal means of number of heat stress days per year for Central Queensland, and HLI upper limit of 86.

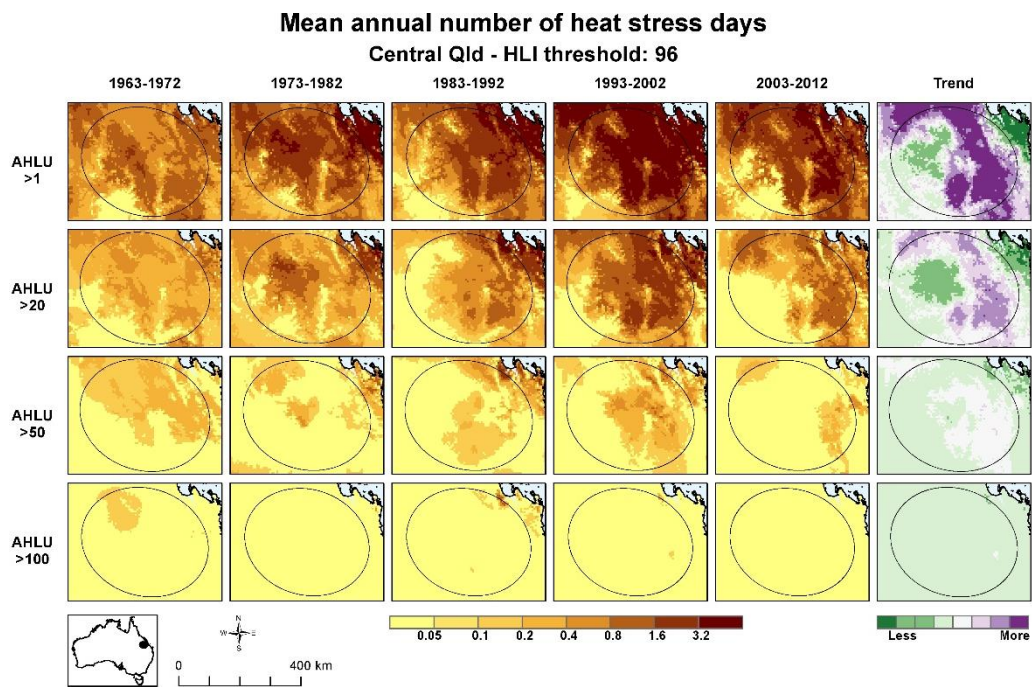


Figure 8. Decadal means of number of heat stress days per year for Central Queensland, and HLI upper limit of 96.

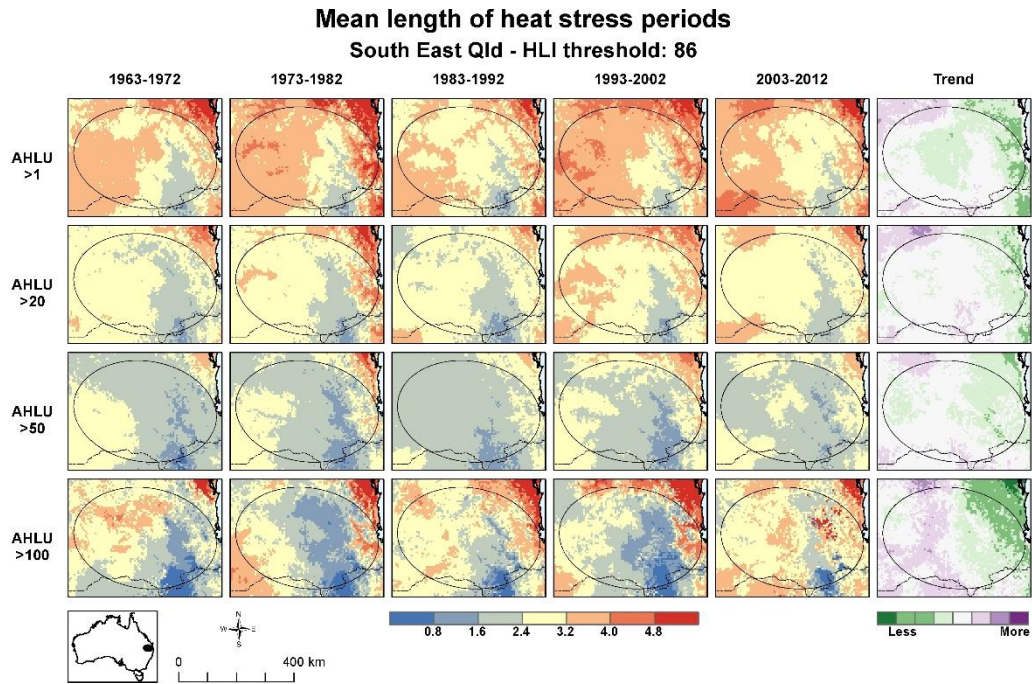


Figure 9. Decadal means of length of consecutive periods of heat stress for South eastern Queensland, and HLI upper limit of 86.

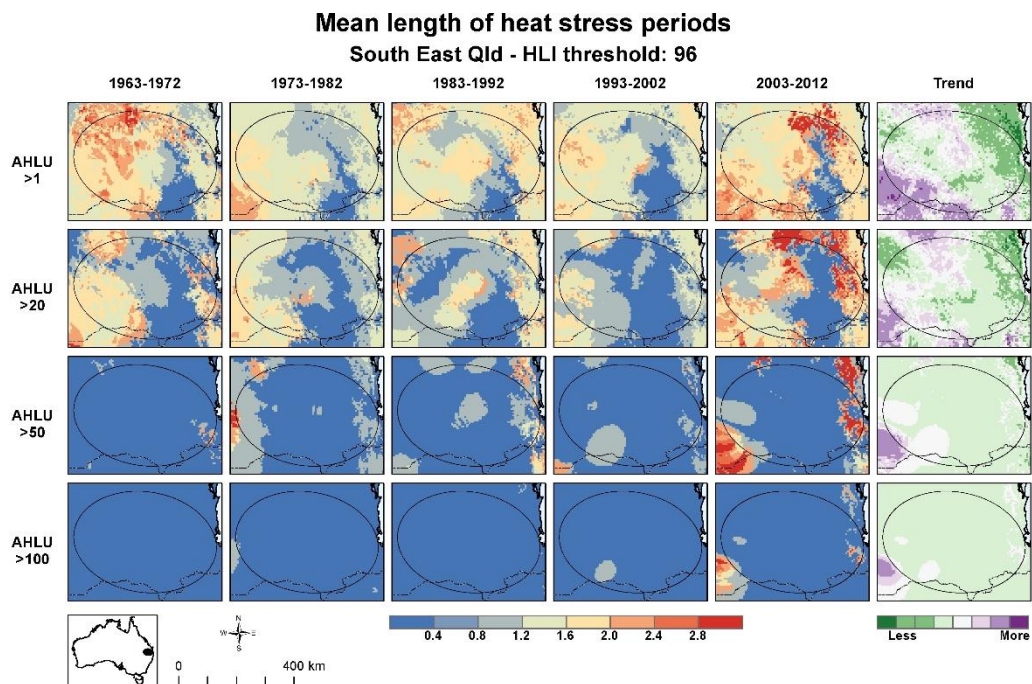


Figure 10. Decadal means of length of consecutive periods of heat stress for South eastern Queensland, and HLI upper limit of 96.

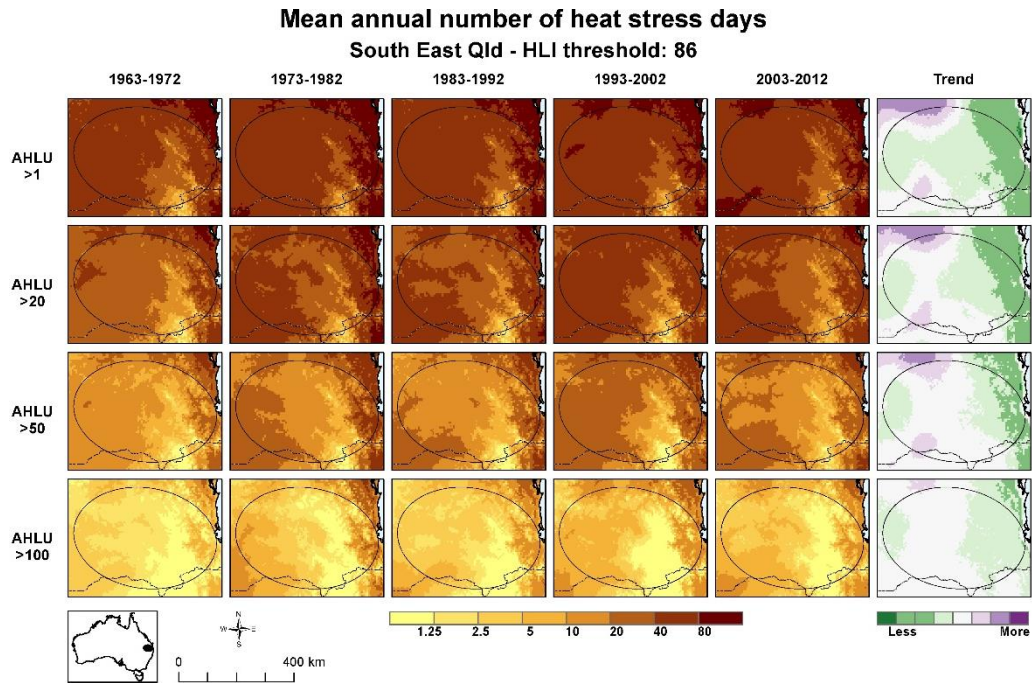


Figure 11. Decadal means of number of heat stress days per year for South eastern Queensland, and HLI upper limit of 86.

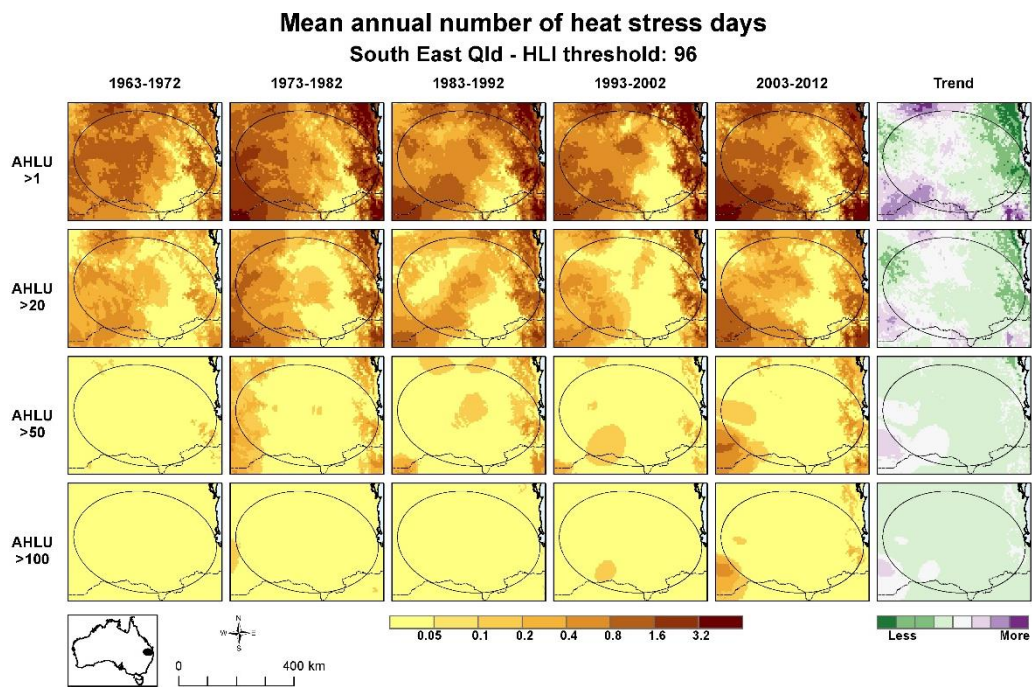


Figure 12. Decadal means of number of heat stress days per year for South eastern Queensland, and HLI upper limit of 96.

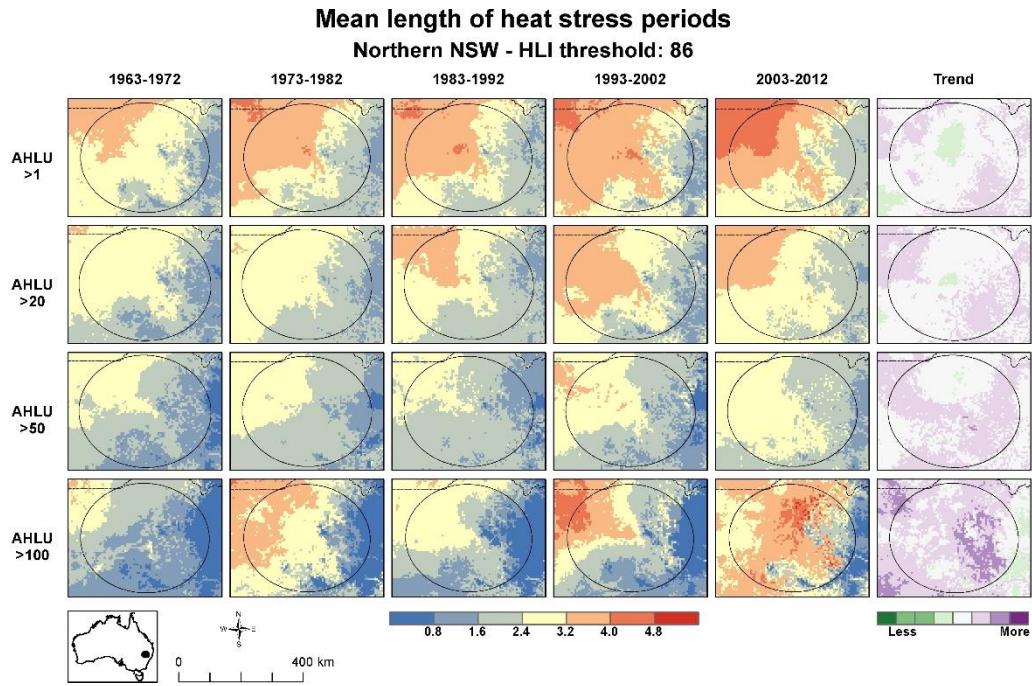


Figure 13. Decadal means of length of consecutive periods of heat stress for Northern New South Wales, and HLI upper limit of 86.

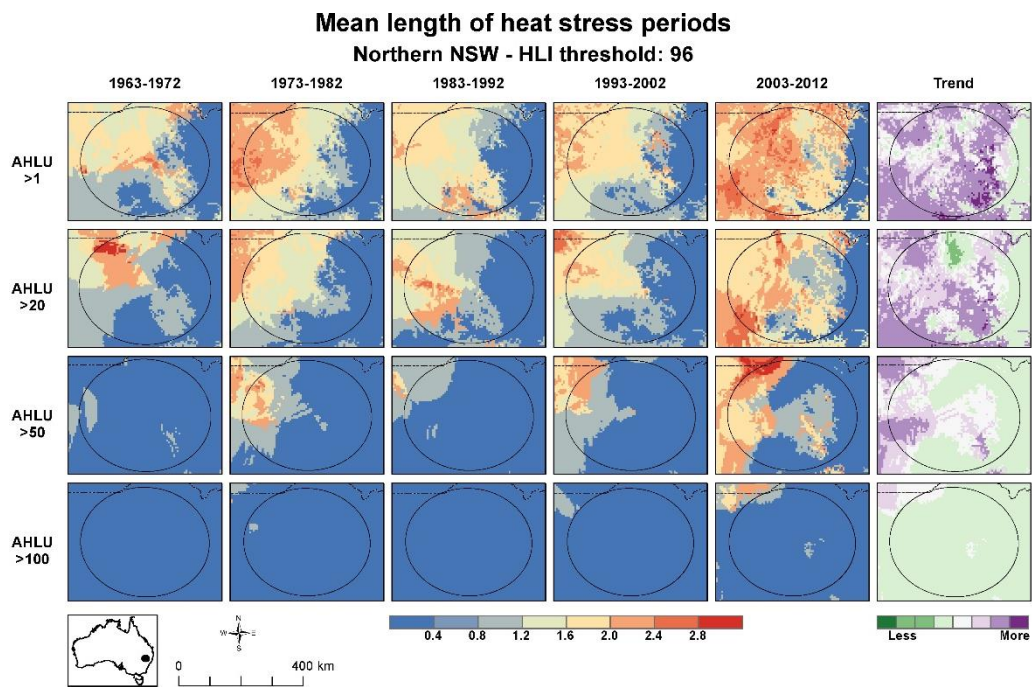


Figure 14. Decadal means of length of consecutive periods of heat stress for Northern New South Wales, and HLI upper limit of 96.

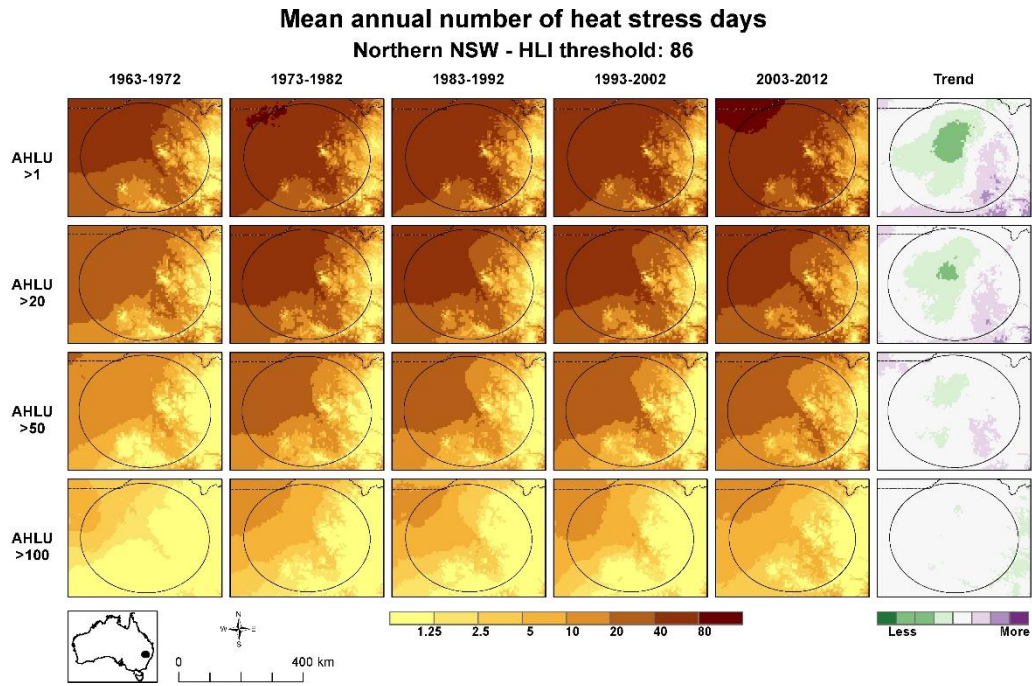


Figure 15. Decadal means of number of heat stress days per year for Northern New South Wales, and HLI upper limit of 86.

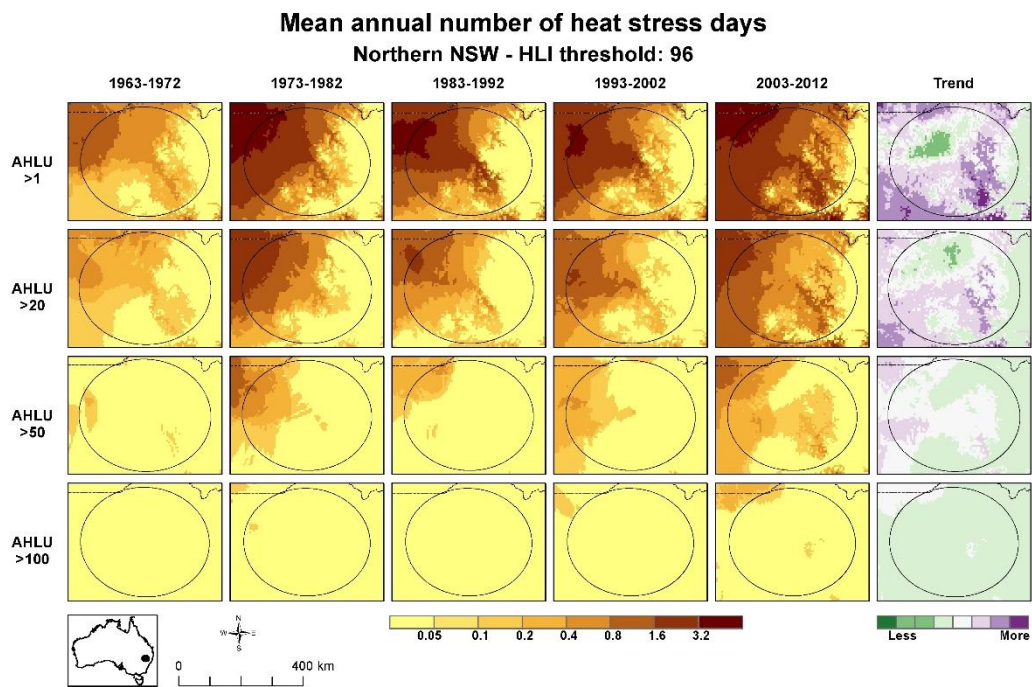


Figure 16. Decadal means of number of heat stress days per year for Northern New South Wales, and HLI upper limit of 96.

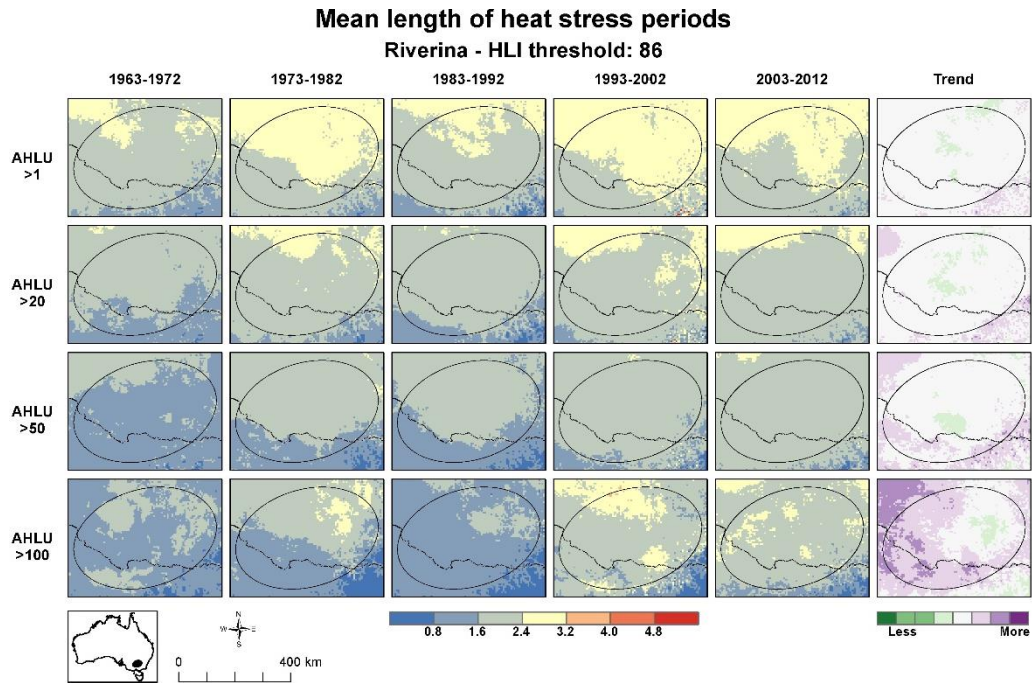


Figure 17. Decadal means of length of consecutive periods of heat stress for Riverina, and HLI upper limit of 86.

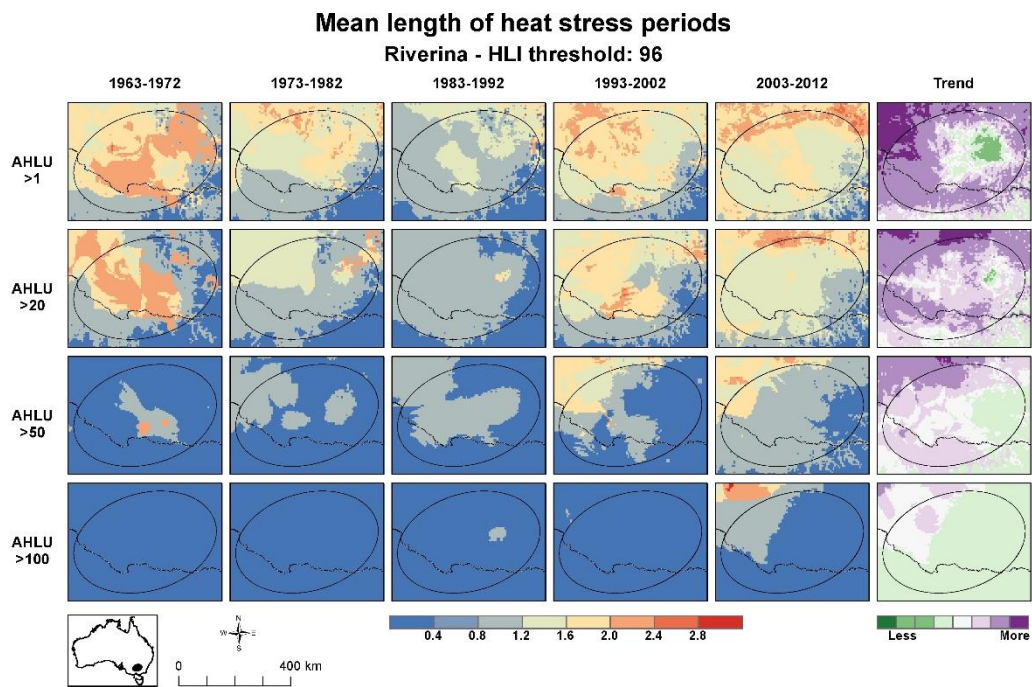


Figure 18. Decadal means of length of consecutive periods of heat stress for Riverina, and HLI upper limit of 96.

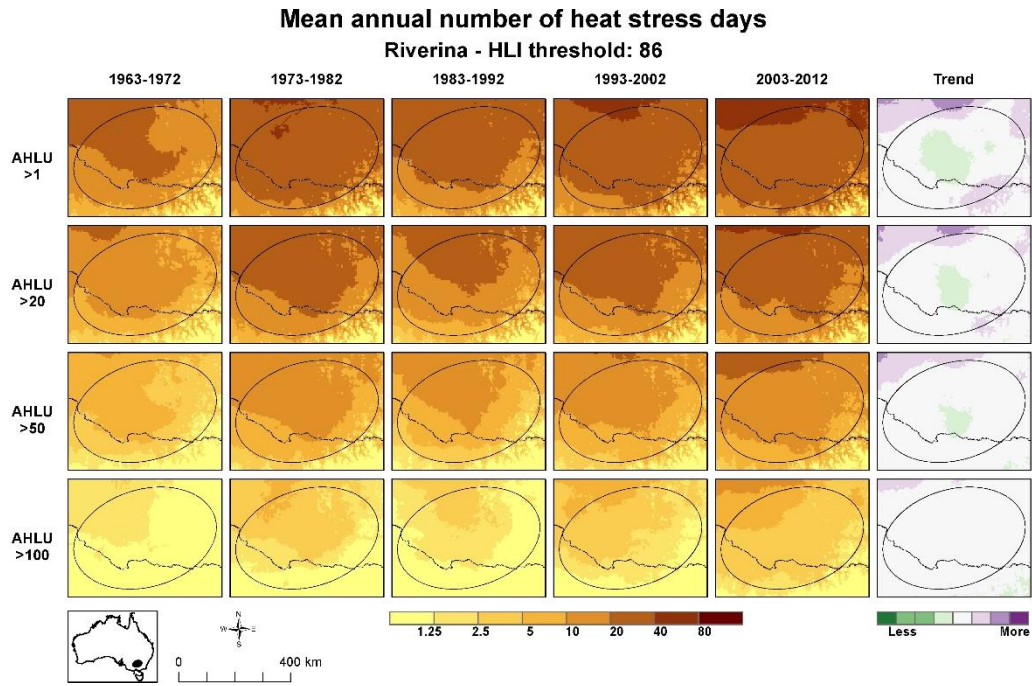


Figure 19. Decadal means of number of heat stress days per year for Riverina, and HLI upper limit of 86.

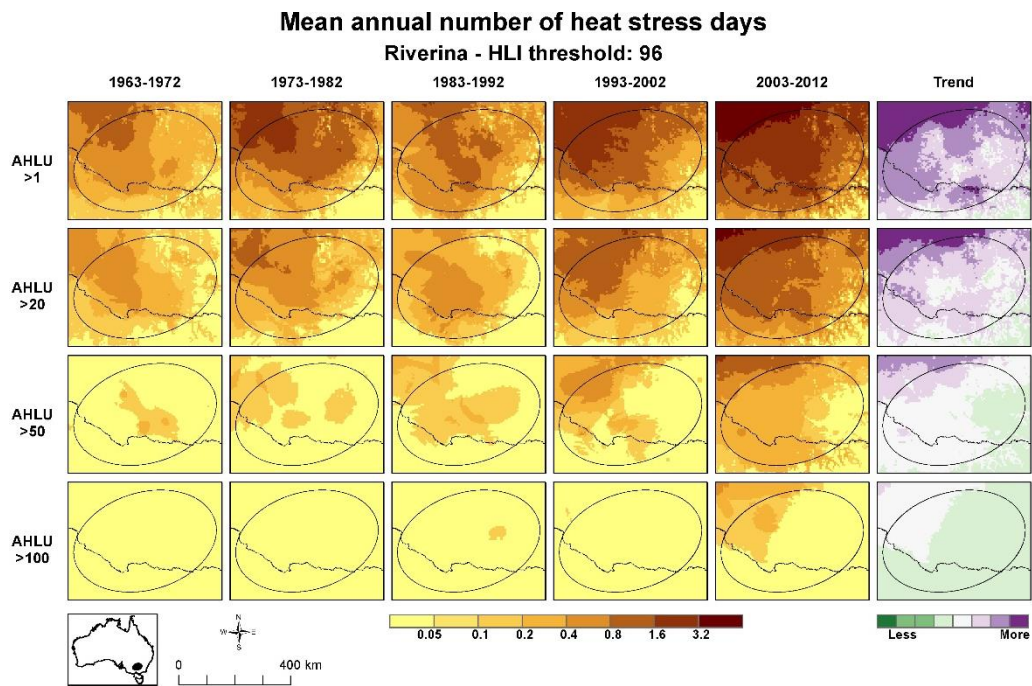


Figure 20. Decadal means of number of heat stress days per year for Riverina, and HLI upper limit of 96.

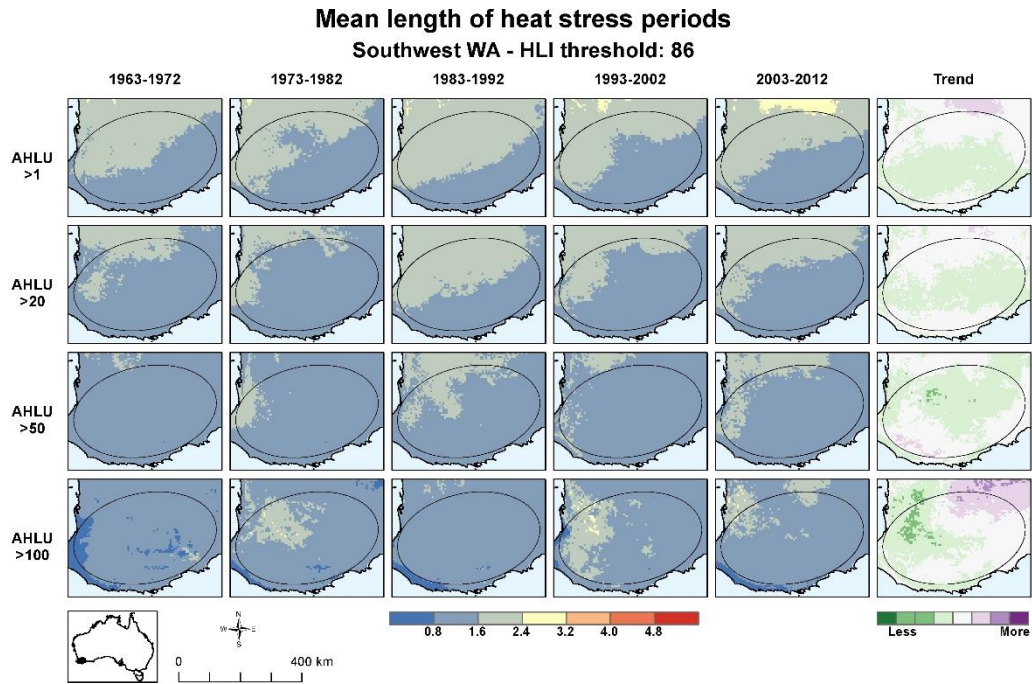


Figure 21. Decadal means of length of consecutive periods of heat stress for Southwest Western Australia, and HLI upper limit of 86.

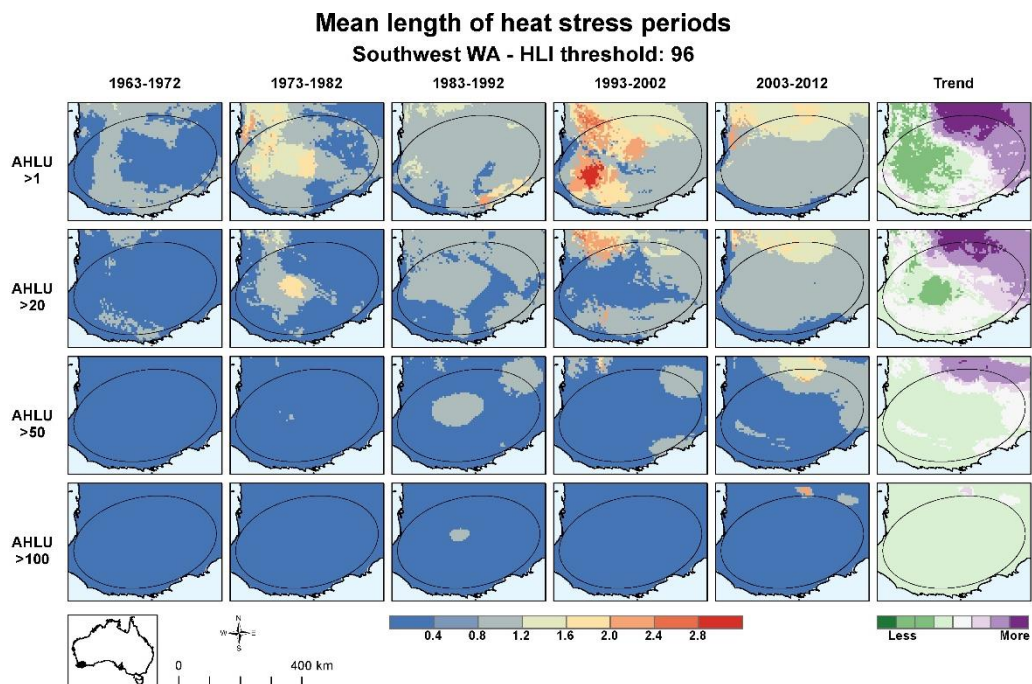


Figure 22. Decadal means of length of consecutive periods of heat stress for Southwest Western Australia, and HLI upper limit of 96.

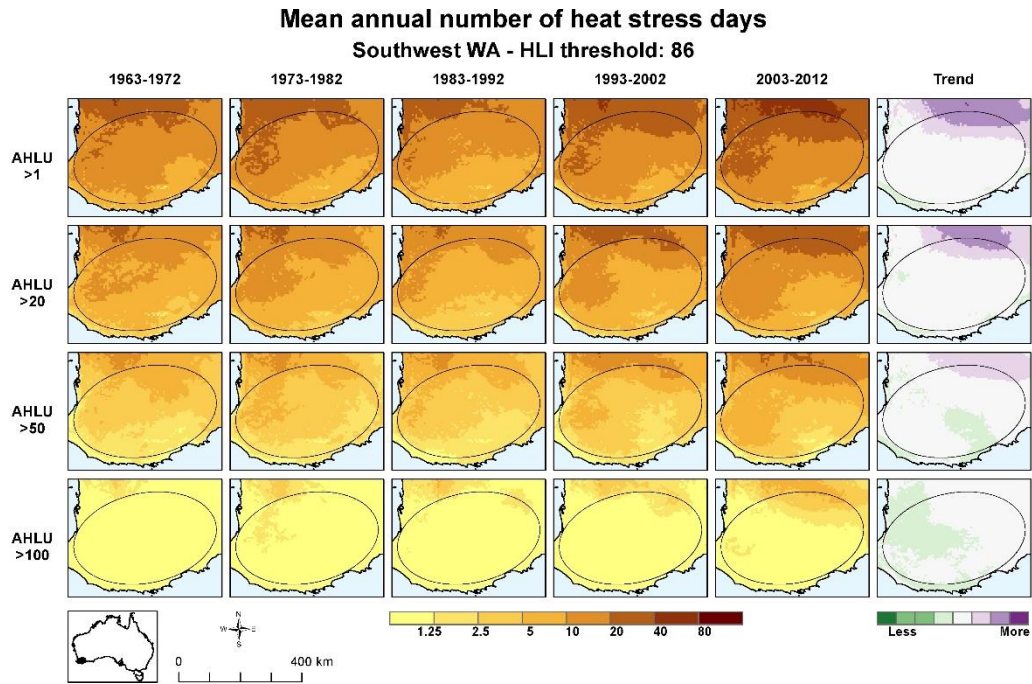


Figure 23. Decadal means of number of heat stress days per year for Southwest Western Australia, and HLI upper limit of 86.

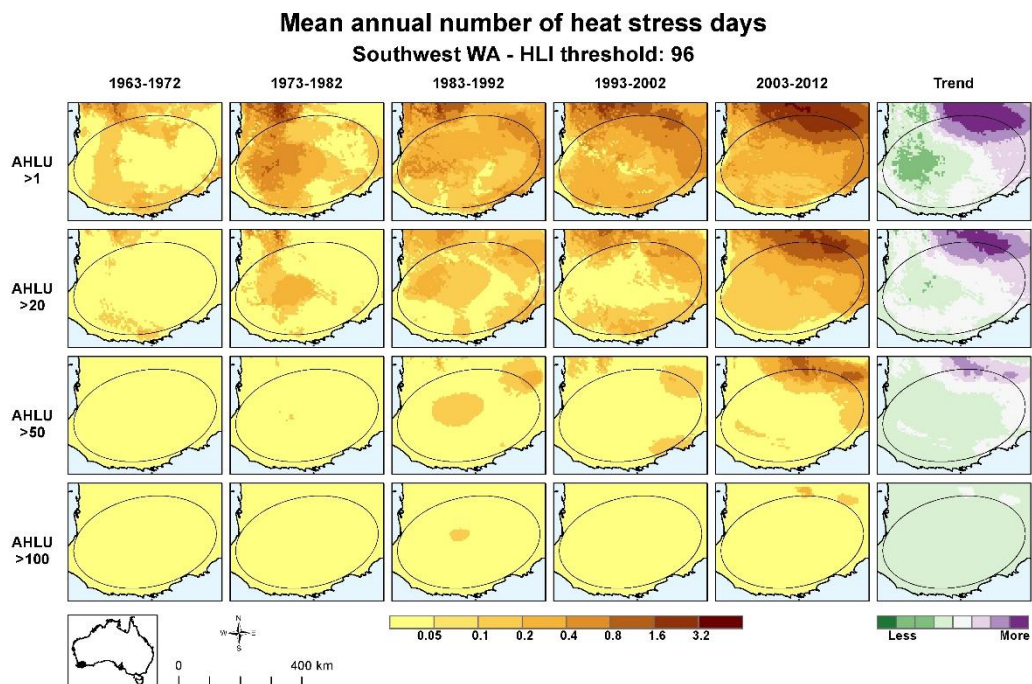


Figure 24. Decadal means of number of heat stress days per year for Southwest Western Australia, and HLI upper limit of 96.

Appendix 4 – Maps of future scenario heat stress³⁹

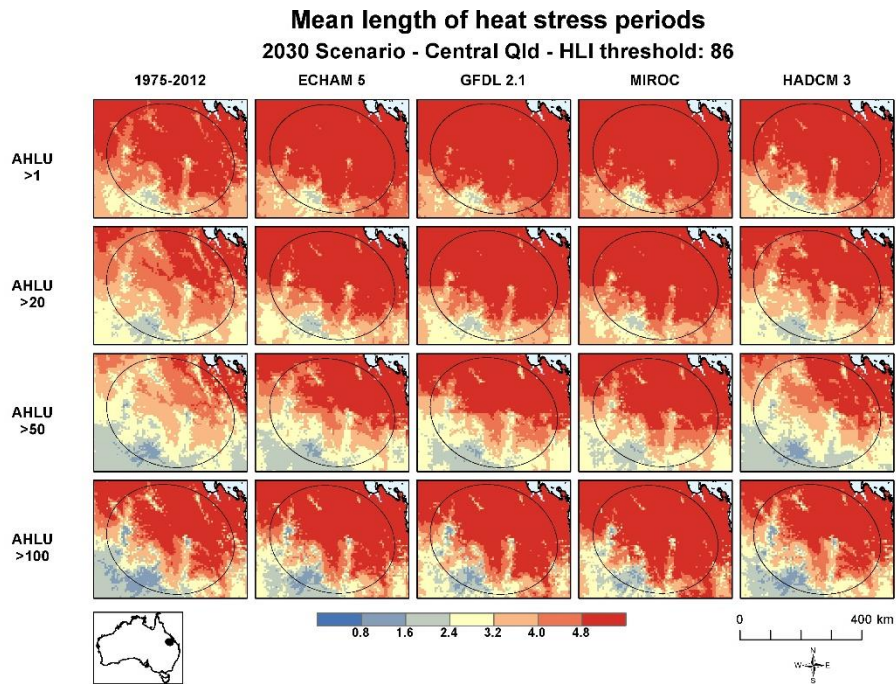


Figure 25. Central Queensland maps of historical (1975-2012) and 2030 GCM scenarios showing mean of length of consecutive periods of heat stress for cattle with HLI upper limit of 86.

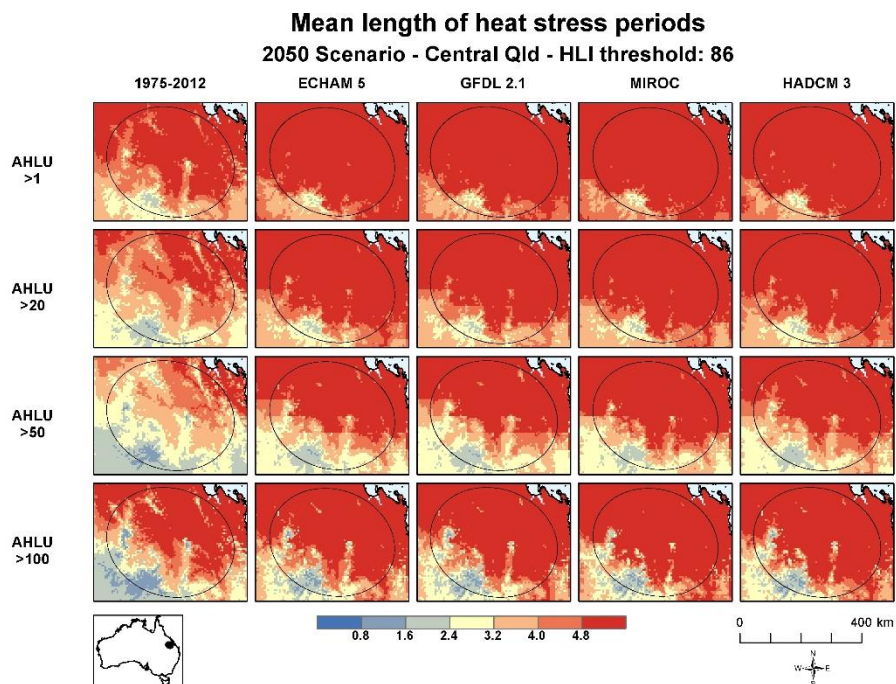


Figure 26. Central Queensland maps of historical (1975-2012) and 2050 GCM scenarios showing mean of length of consecutive periods of heat stress for cattle with HLI upper limit of 86.

³⁹ Note that linear and square artefacts that appear in some of the maps are an unavoidable consequence of the application of the 0.5° spatial resolution GCM data to the 0.05° historical data.

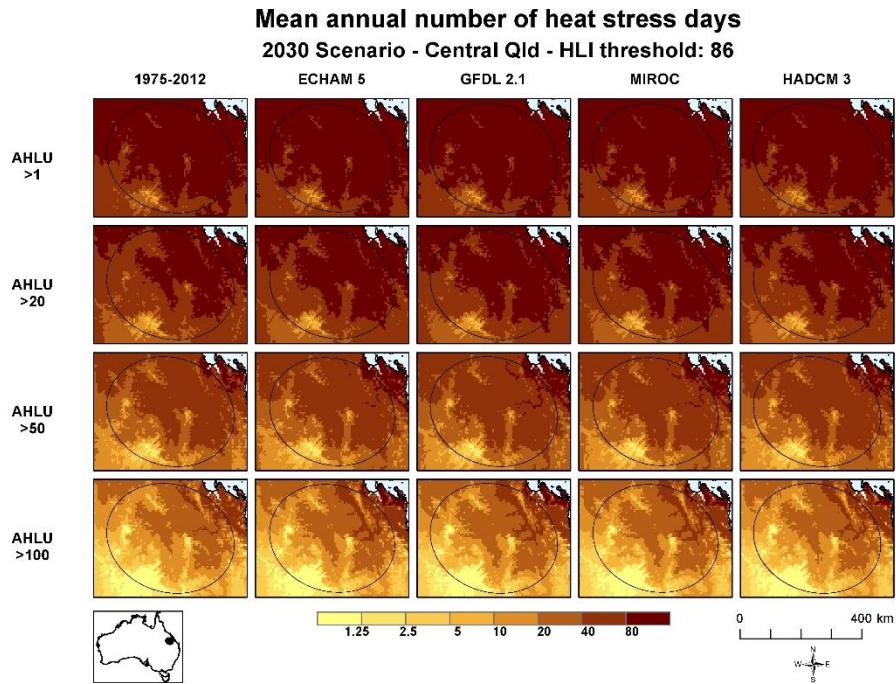


Figure 27. Central Queensland maps of historical (1975-2012) and 2030 GCM scenarios showing mean of number of heat stress days per year for cattle with HLI upper limit of 86.

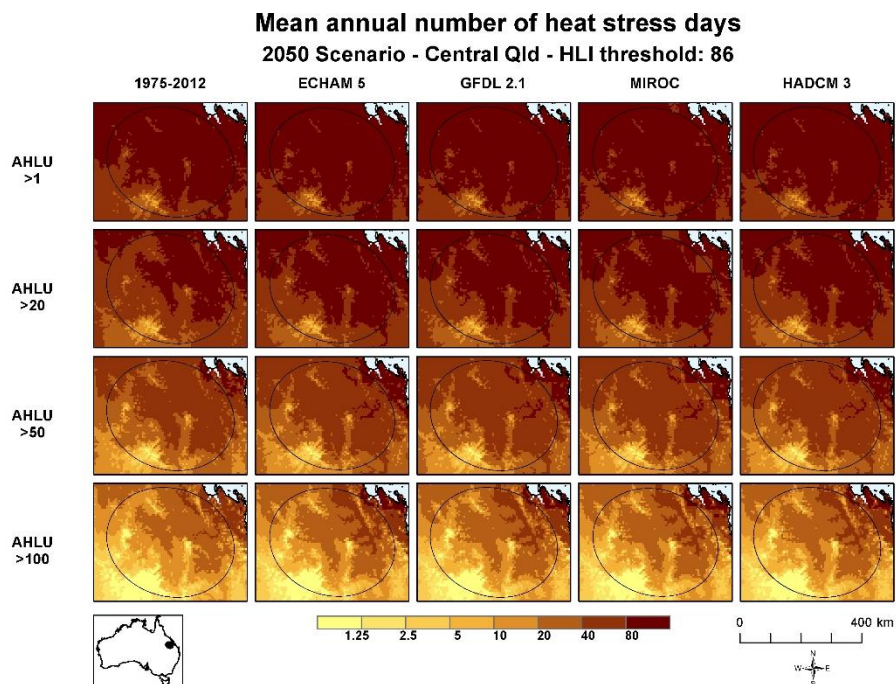


Figure 28. Central Queensland maps of historical (1975-2012) and 2050 GCM scenarios showing mean of number of heat stress days per year for cattle with HLI upper limit of 86.

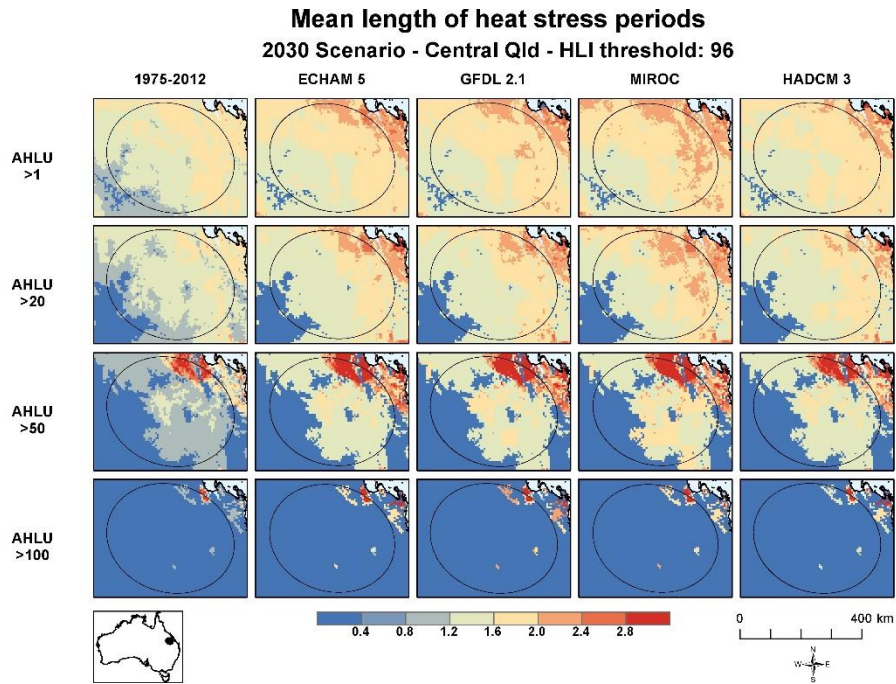


Figure 29. Central Queensland maps of historical (1975-2012) and 2030 GCM scenarios showing mean of length of consecutive periods of heat stress for cattle with HLI upper limit of 96.

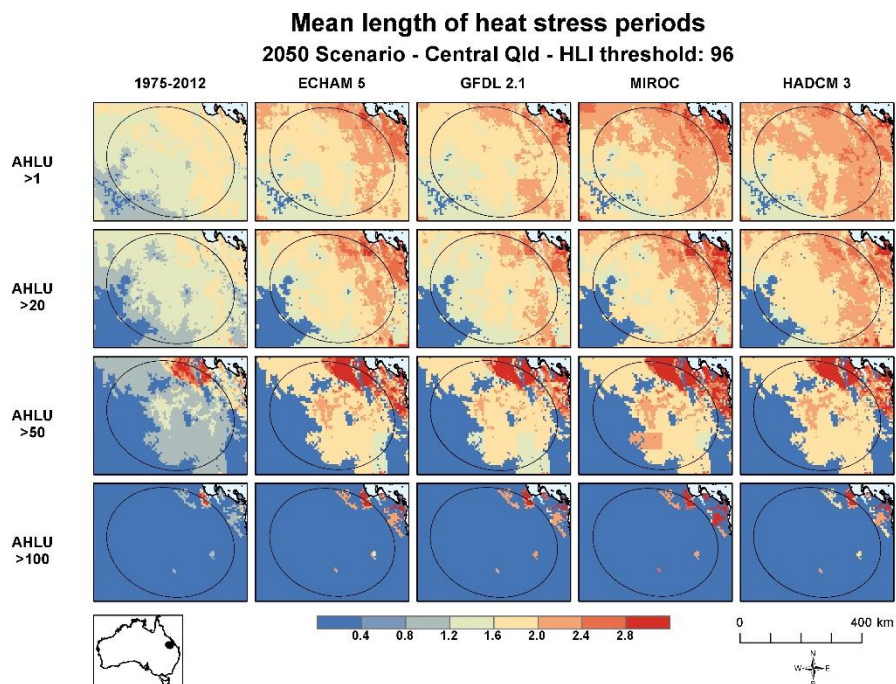


Figure 30. Central Queensland maps of historical (1975-2012) and 2050 GCM scenarios showing mean of length of consecutive periods of heat stress for cattle with HLI upper limit of 96.

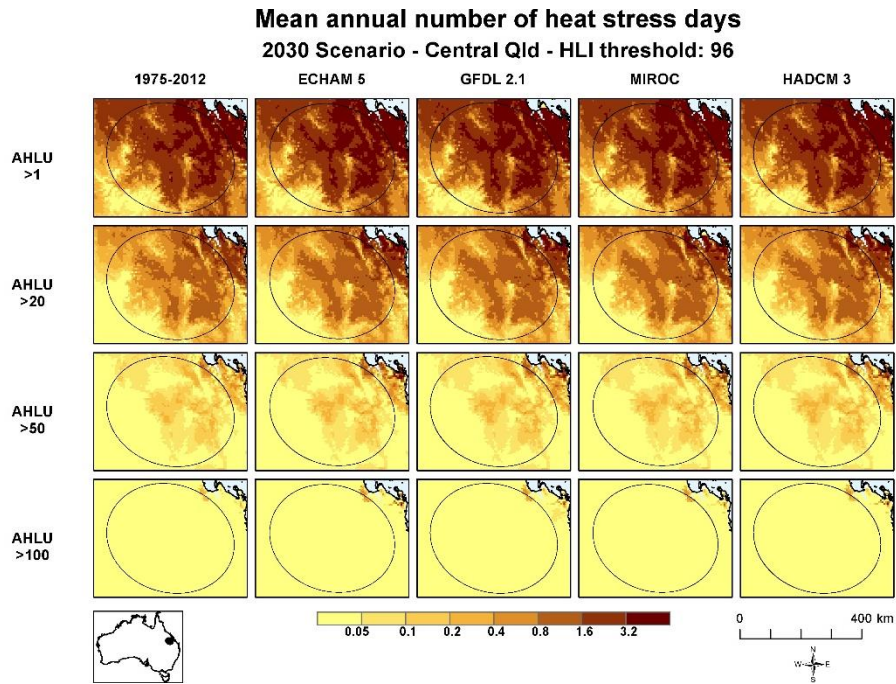


Figure 31. Central Queensland maps of historical (1975-2012) and 2030 GCM scenarios showing mean of number of heat stress days per year for cattle with HLI upper limit of 96.

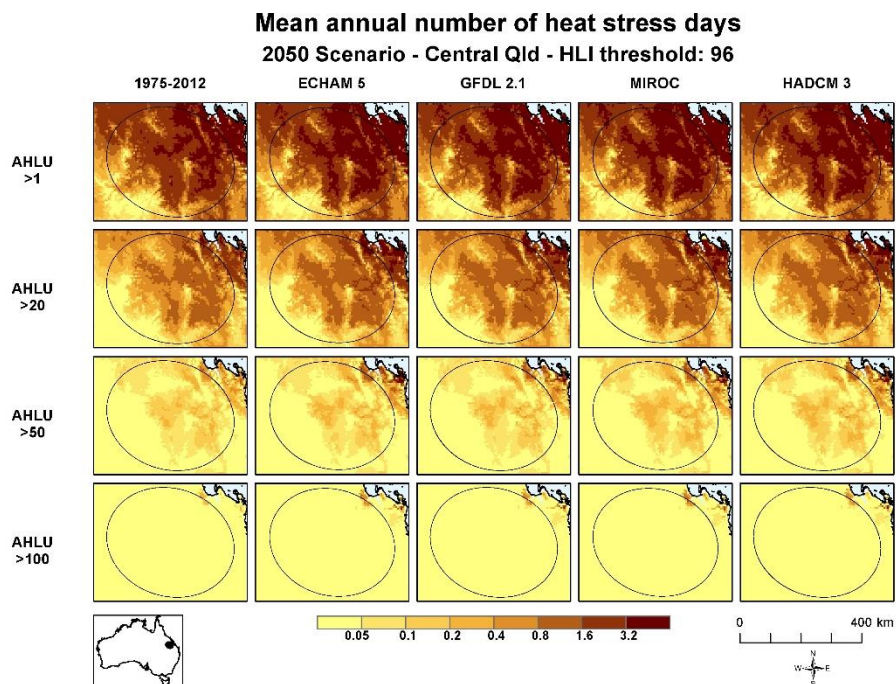


Figure 32. Central Queensland maps of historical (1975-2012) and 2050 GCM scenarios showing mean of number of heat stress days per year for cattle with HLI upper limit of 96.

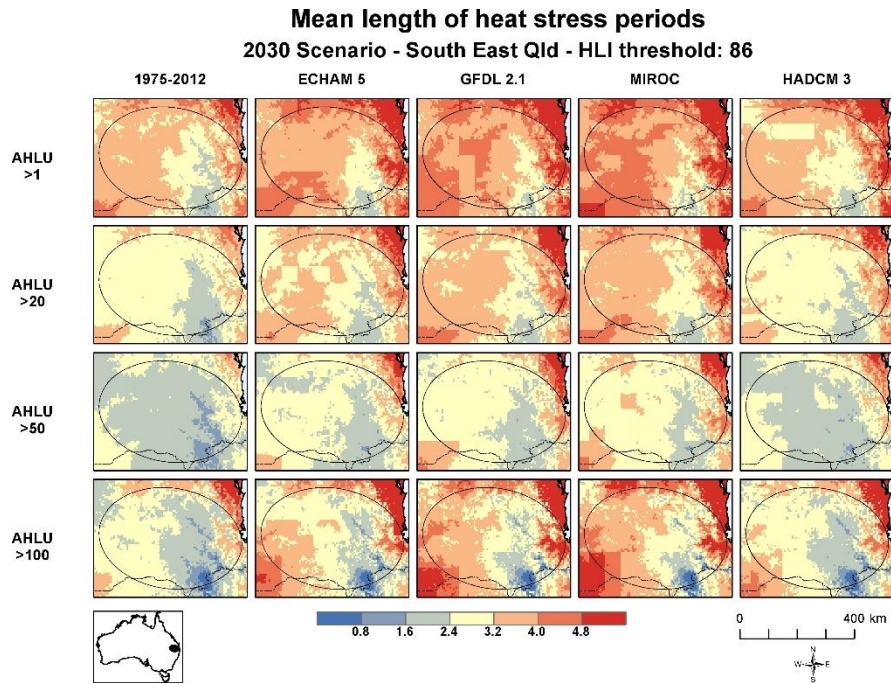


Figure 33. South eastern Queensland maps of historical (1975-2012) and 2030 GCM scenarios showing mean of length of consecutive periods of heat stress for cattle with HLI upper limit of 86.

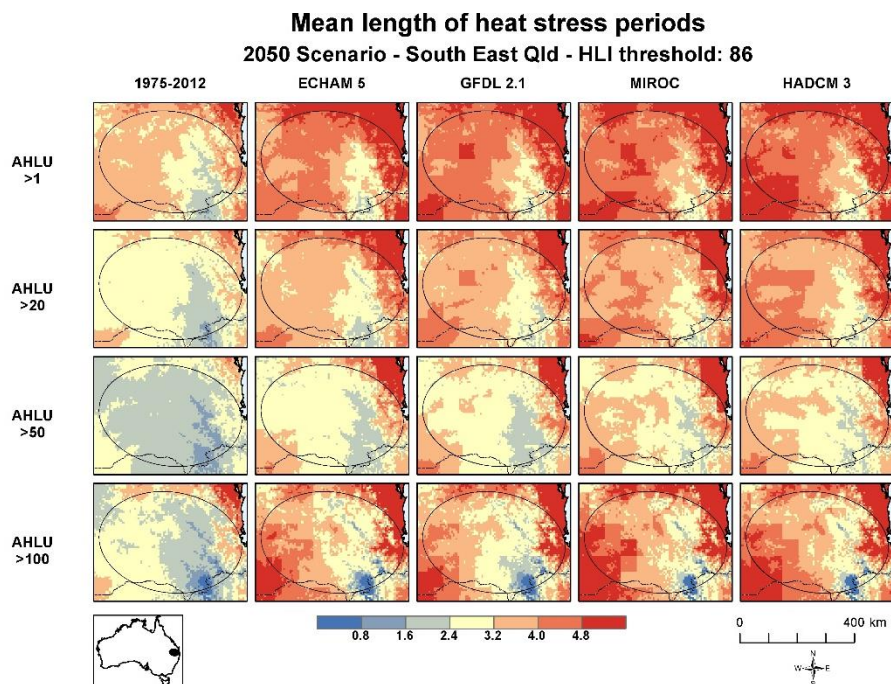


Figure 34. South eastern Queensland maps of historical (1975-2012) and 2050 GCM scenarios showing mean of length of consecutive periods of heat stress for cattle with HLI upper limit of 86.

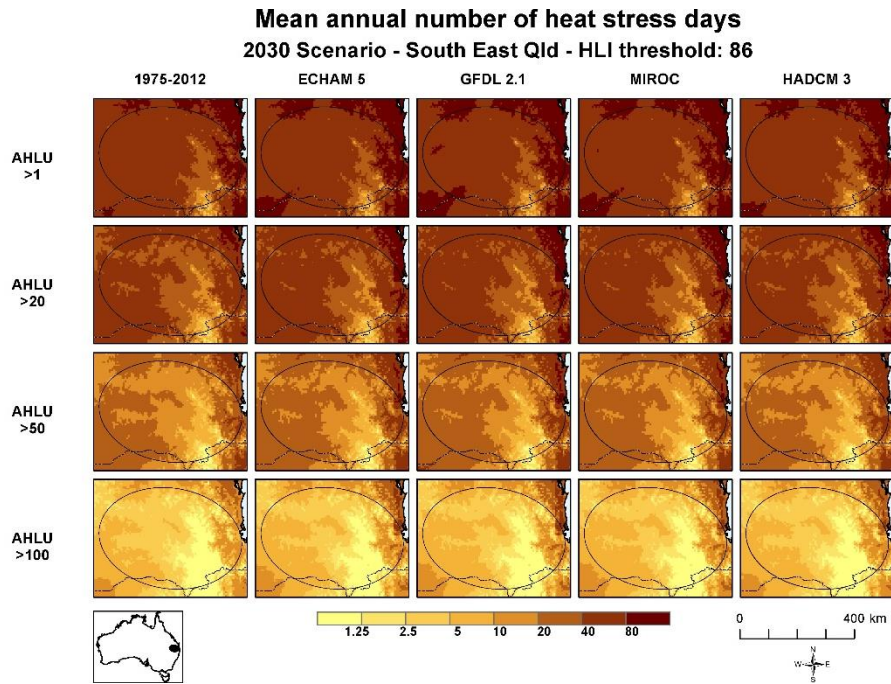


Figure 35. South eastern Queensland maps of historical (1975-2012) and 2030 GCM scenarios showing mean of number of heat stress days per year for cattle with HLI upper limit of 86.

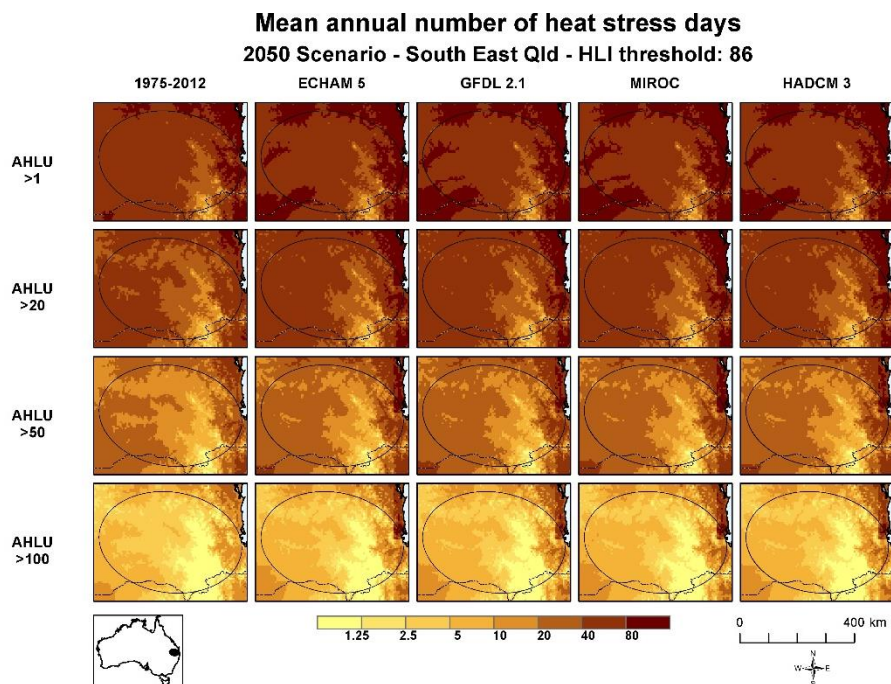


Figure 36. South eastern Queensland maps of historical (1975-2012) and 2050 GCM scenarios showing mean of number of heat stress days per year for cattle with HLI upper limit of 86.

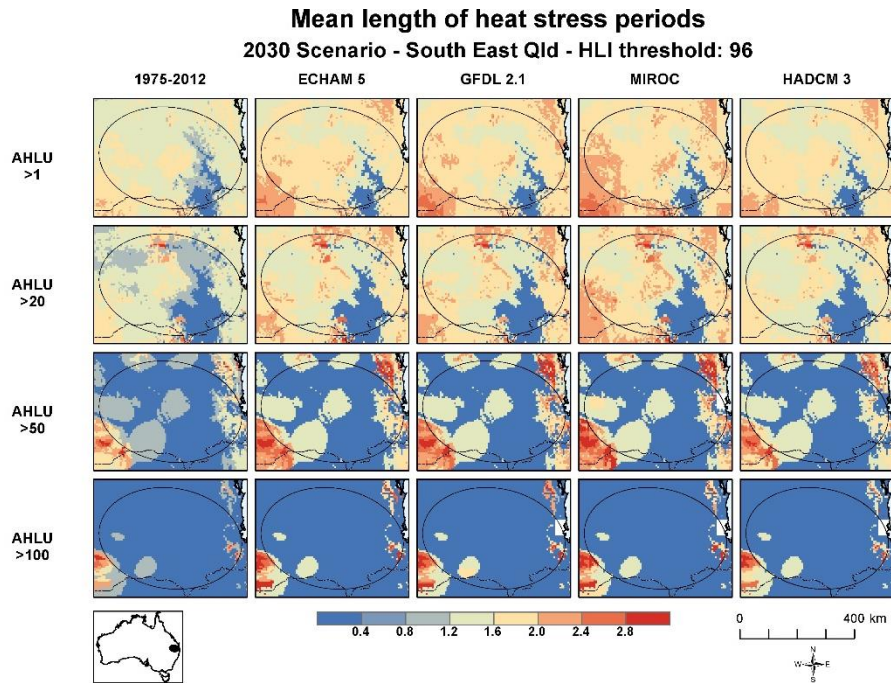


Figure 37. South eastern Queensland maps of historical (1975-2012) and 2030 GCM scenarios showing mean of length of consecutive periods of heat stress for cattle with HLI upper limit of 96.

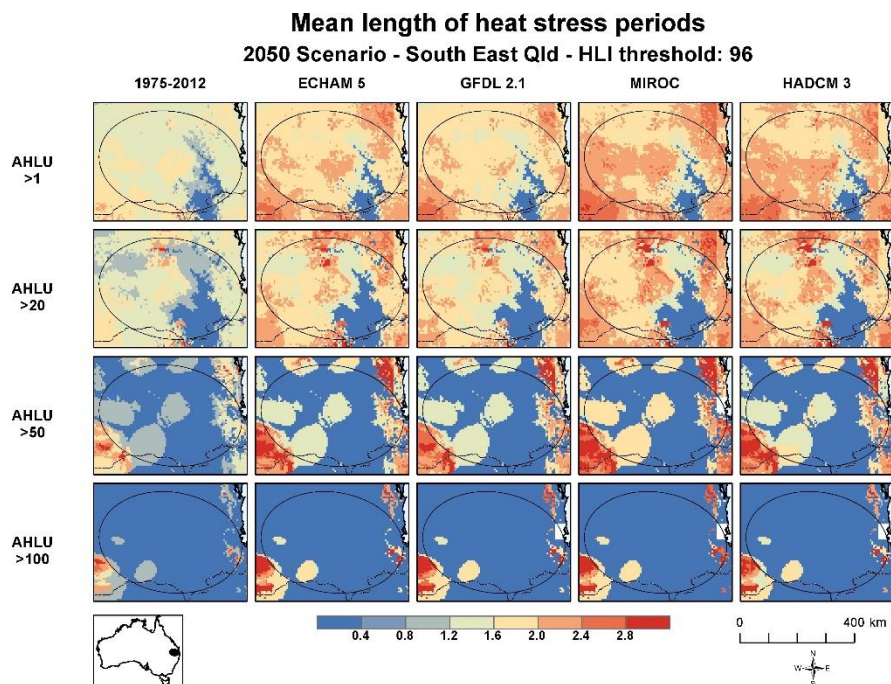


Figure 38. South eastern Queensland maps of historical (1975-2012) and 2050 GCM scenarios showing mean of length of consecutive periods of heat stress for cattle with HLI upper limit of 96.

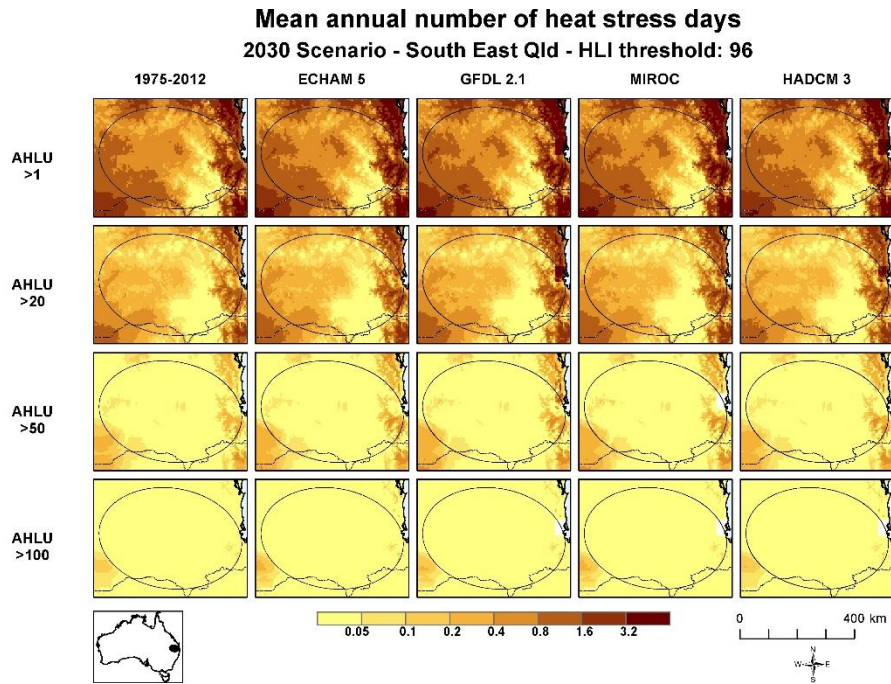


Figure 39. South eastern Queensland maps of historical (1975-2012) and 2030 GCM scenarios showing mean of number of heat stress days per year for cattle with HLI upper limit of 96.

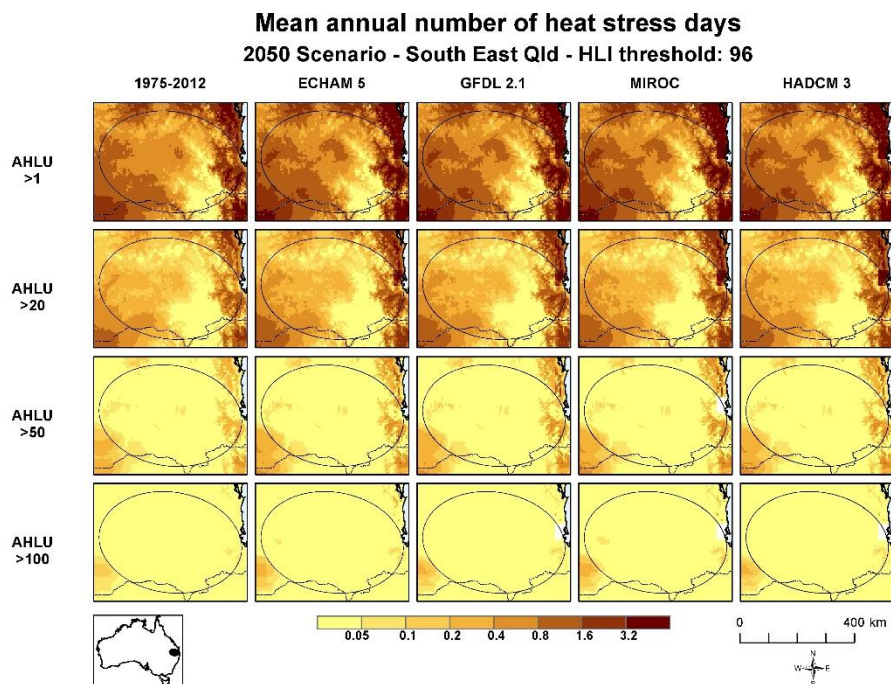


Figure 40. South eastern Queensland maps of historical (1975-2012) and 2050 GCM scenarios showing mean of number of heat stress days per year for cattle with HLI upper limit of 96.

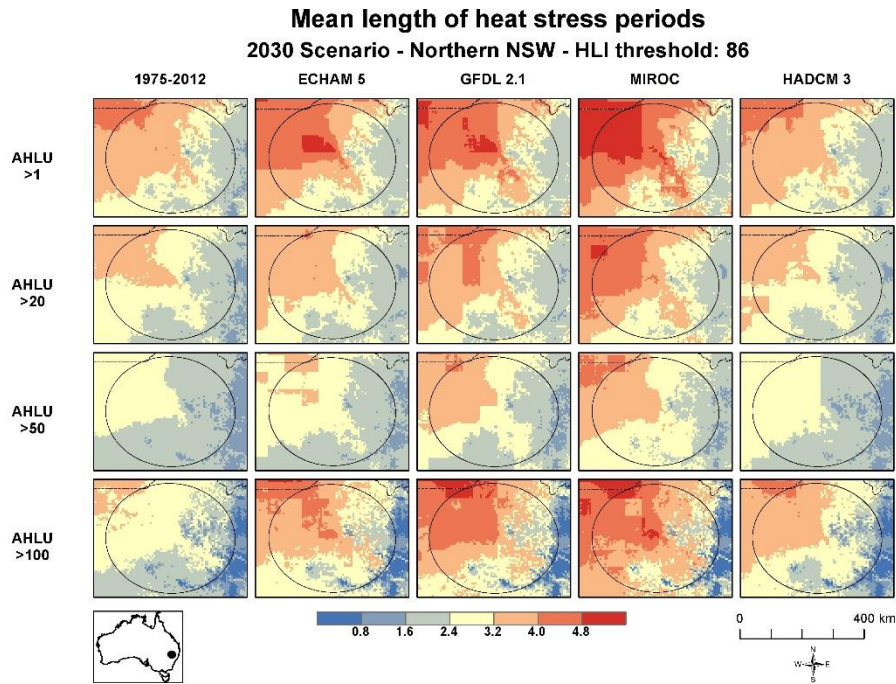


Figure 41. Northern New South Wales maps of historical (1975-2012) and 2030 GCM scenarios showing mean of length of consecutive periods of heat stress for cattle with HLI upper limit of 86.

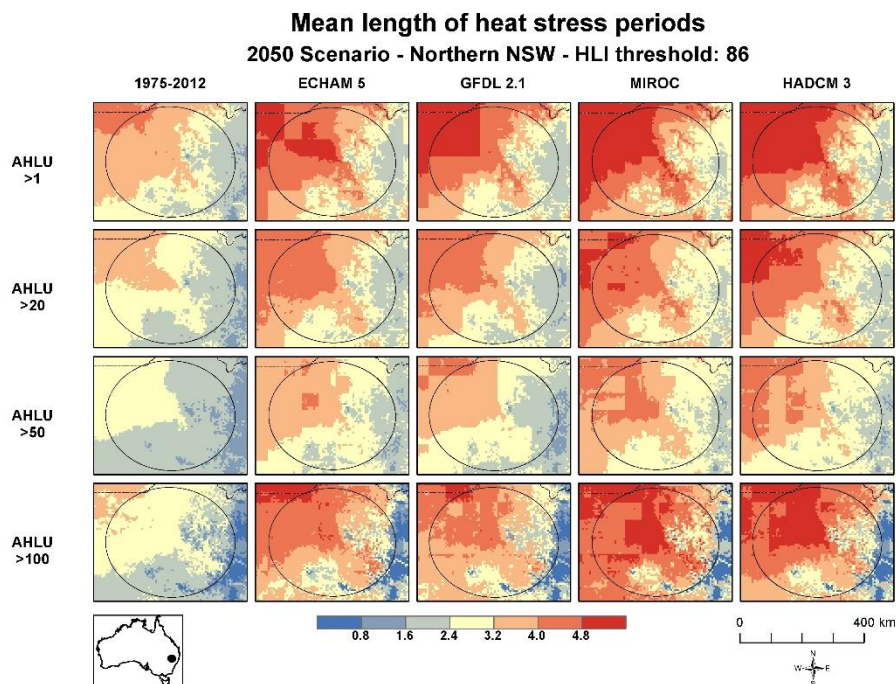


Figure 42. Northern New South Wales maps of historical (1975-2012) and 2050 GCM scenarios showing mean of length of consecutive periods of heat stress for cattle with HLI upper limit of 86.

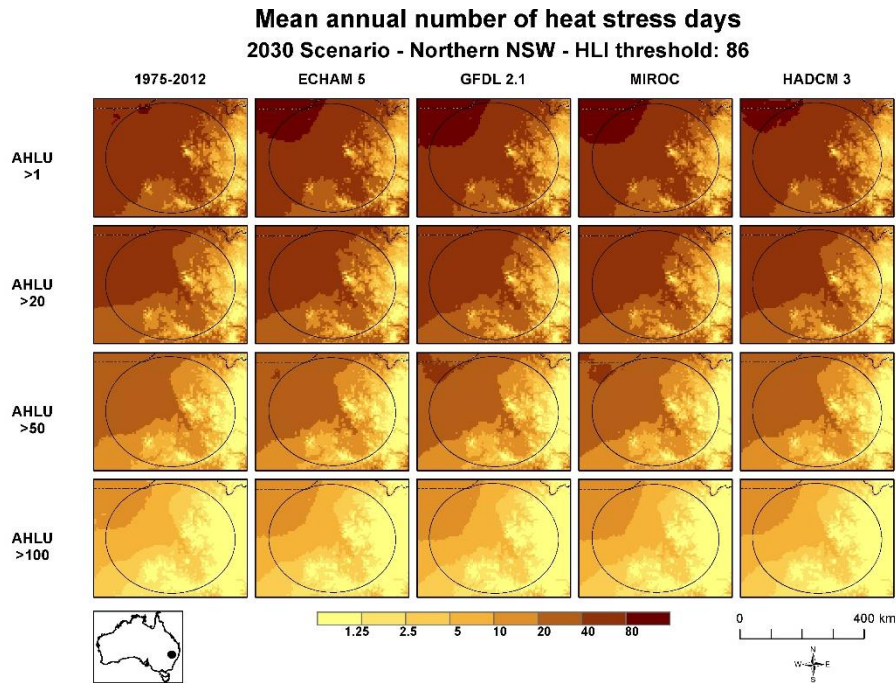


Figure 43. Northern New South Wales maps of historical (1975-2012) and 2030 GCM scenarios showing mean of number of heat stress days per year for cattle with HLI upper limit of 86.

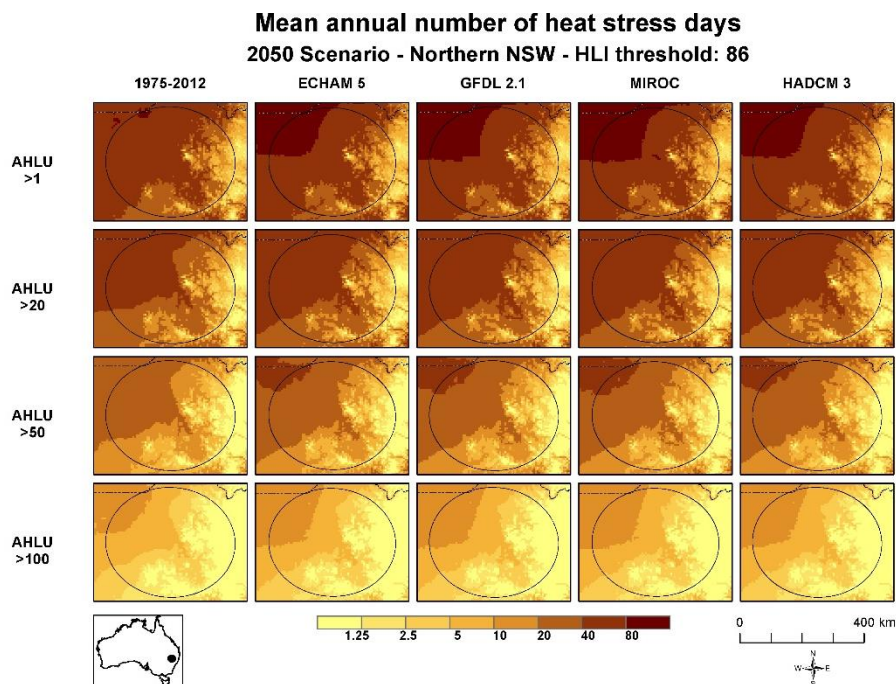


Figure 44. Northern New South Wales maps of historical (1975-2012) and 2050 GCM scenarios showing mean of number of heat stress days per year for cattle with HLI upper limit of 86.

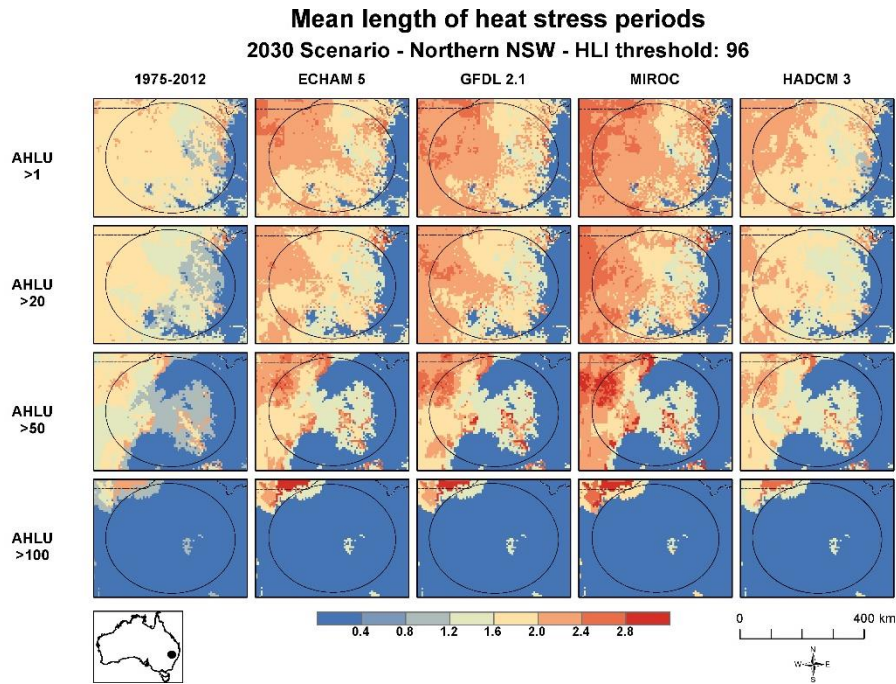


Figure 45. Northern New South Wales maps of historical (1975-2012) and 2030 GCM scenarios showing mean of length of consecutive periods of heat stress for cattle with HLI upper limit of 96.

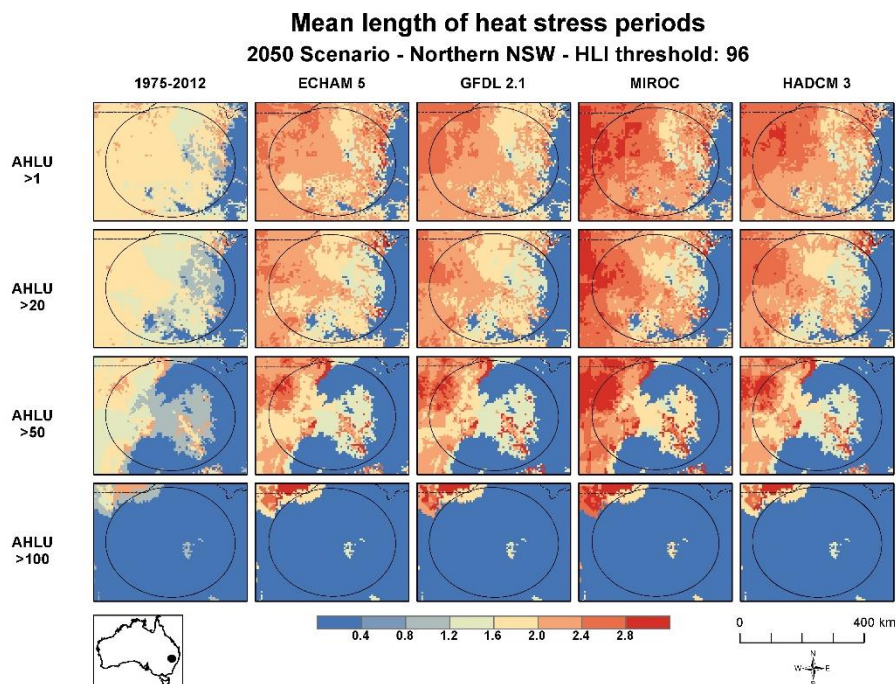


Figure 46. Northern New South Wales maps of historical (1975-2012) and 2050 GCM scenarios showing mean of length of consecutive periods of heat stress for cattle with HLI upper limit of 96.

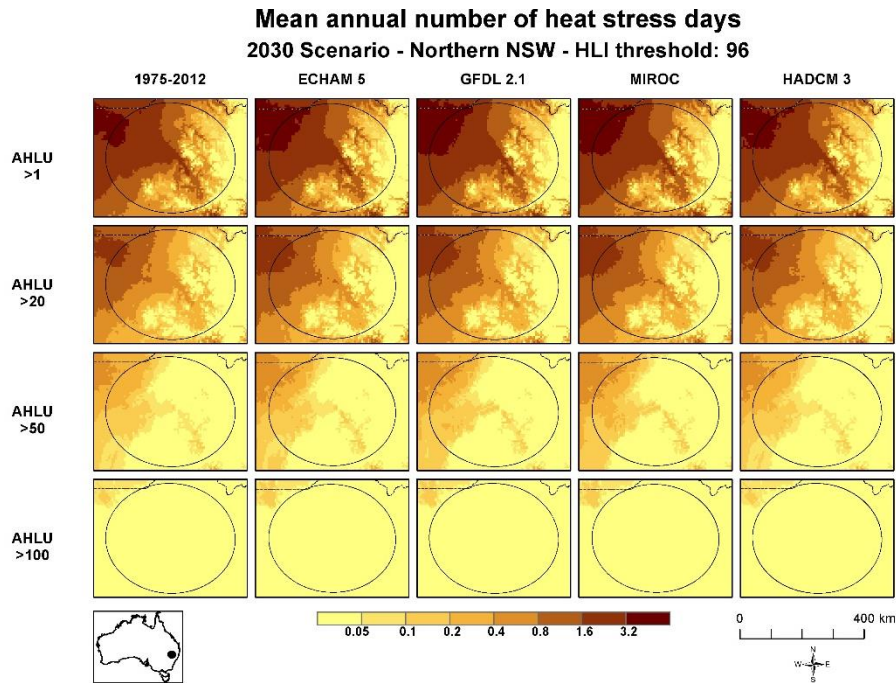


Figure 47. Northern New South Wales maps of historical (1975-2012) and 2030 GCM scenarios showing mean of number of heat stress days per year for cattle with HLI upper limit of 96.

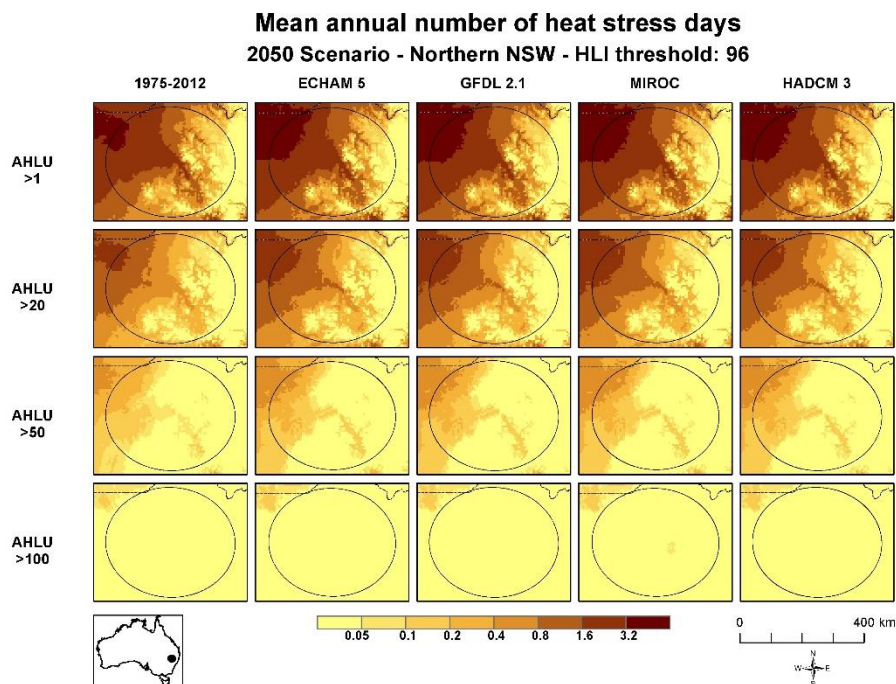


Figure 48. Northern New South Wales maps of historical (1975-2012) and 2050 GCM scenarios showing mean of number of heat stress days per year for cattle with HLI upper limit of 96.

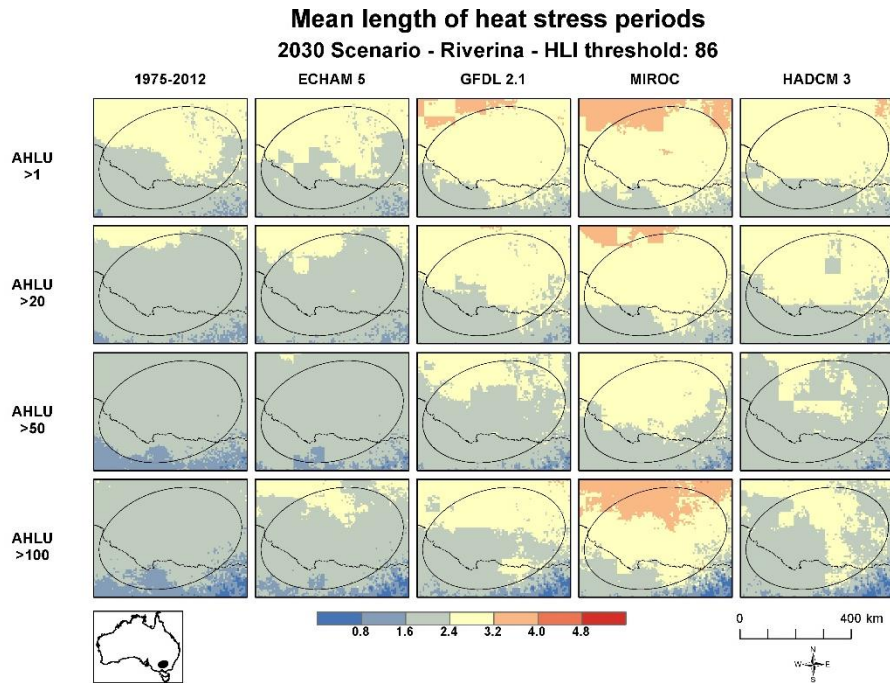


Figure 49. Riverina maps of historical (1975-2012) and 2030 GCM scenarios showing mean of length of consecutive periods of heat stress for cattle with HLI upper limit of 86.

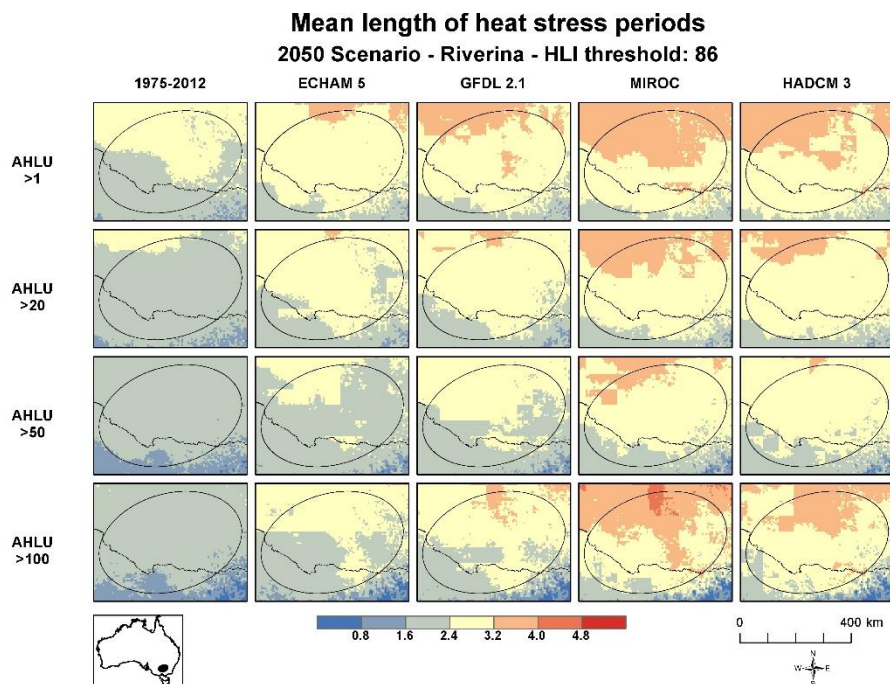


Figure 50. Riverina maps of historical (1975-2012) and 2050 GCM scenarios showing mean of length of consecutive periods of heat stress for cattle with HLI upper limit of 86.

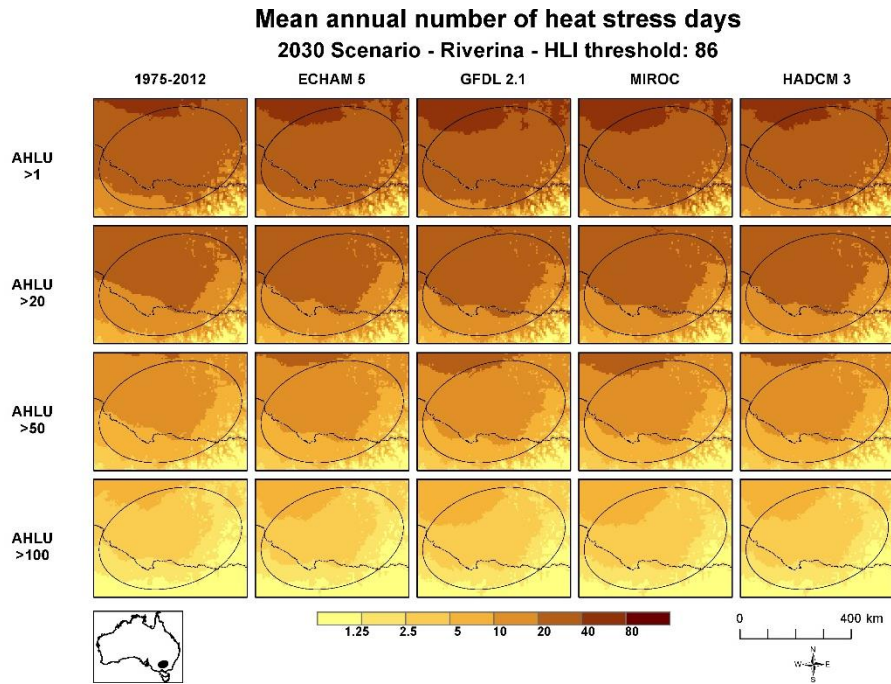


Figure 51. Riverina maps of historical (1975-2012) and 2030 GCM scenarios showing mean of number of heat stress days per year for cattle with HLI upper limit of 86.

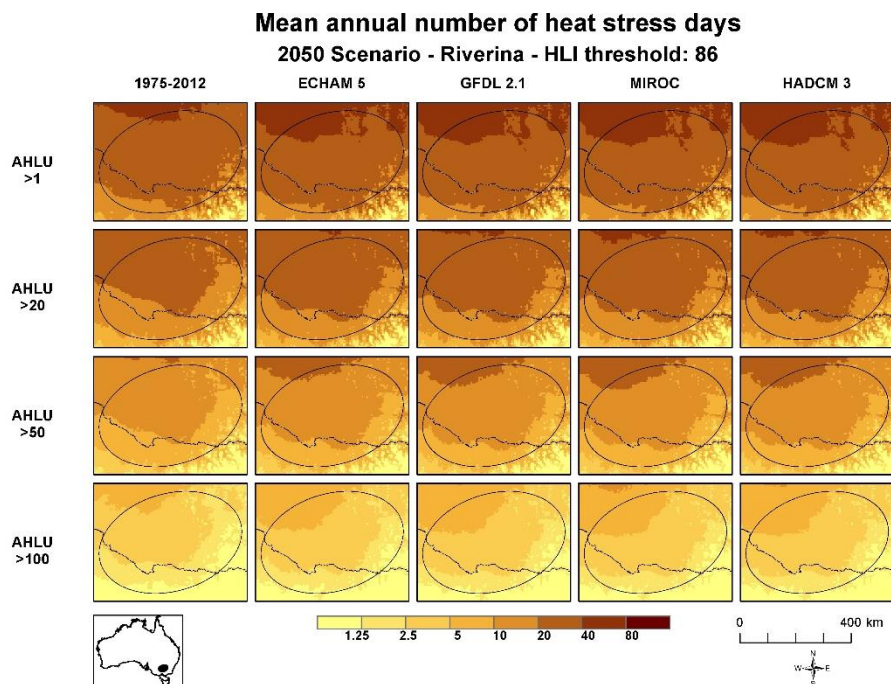


Figure 52. Riverina maps of historical (1975-2012) and 2050 GCM scenarios showing mean of number of heat stress days per year for cattle with HLI upper limit of 86.

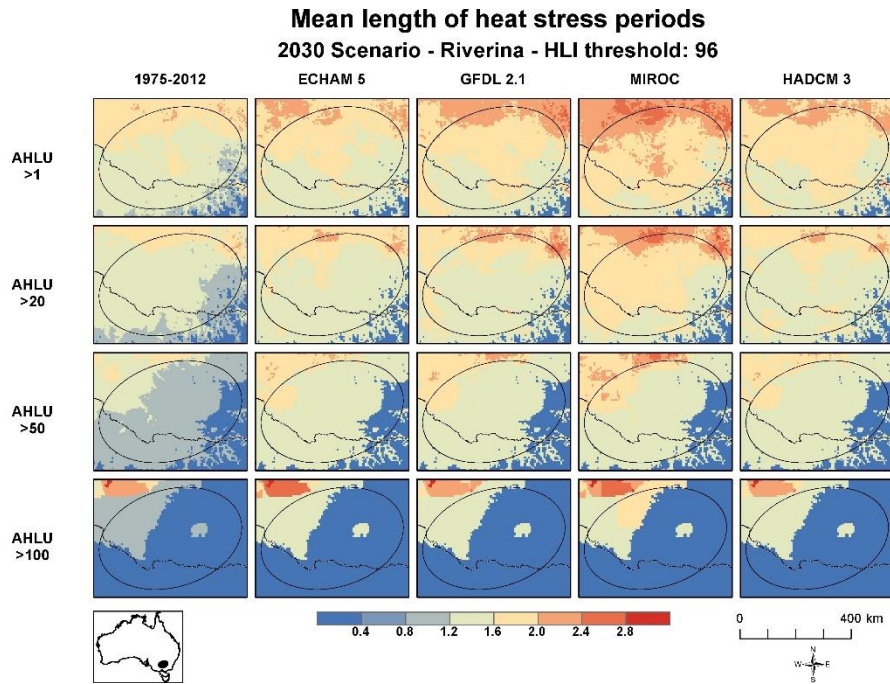


Figure 53. Riverina maps of historical (1975-2012) and 2030 GCM scenarios showing mean of length of consecutive periods of heat stress for cattle with HLI upper limit of 96.

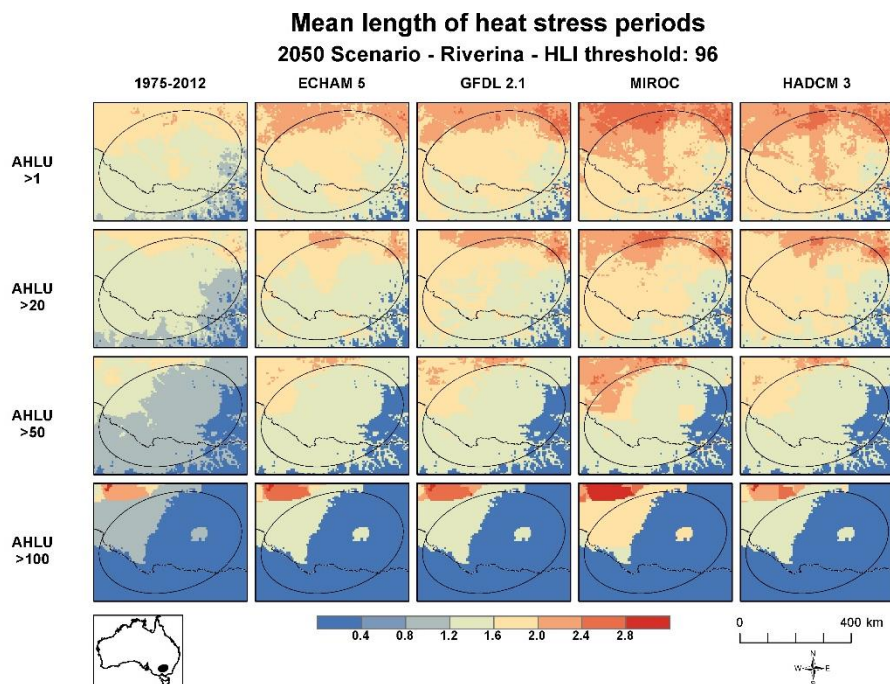


Figure 54. Riverina maps of historical (1975-2012) and 2050 GCM scenarios showing mean of length of consecutive periods of heat stress for cattle with HLI upper limit of 96.

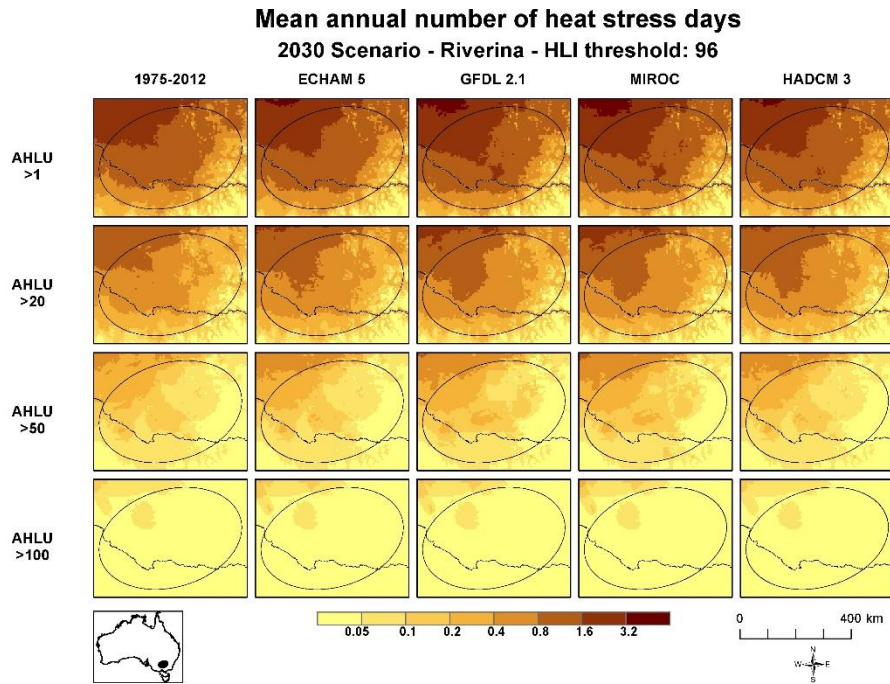


Figure 55. Riverina maps of historical (1975-2012) and 2030 GCM scenarios showing mean of number of heat stress days per year for cattle with HLI upper limit of 96.

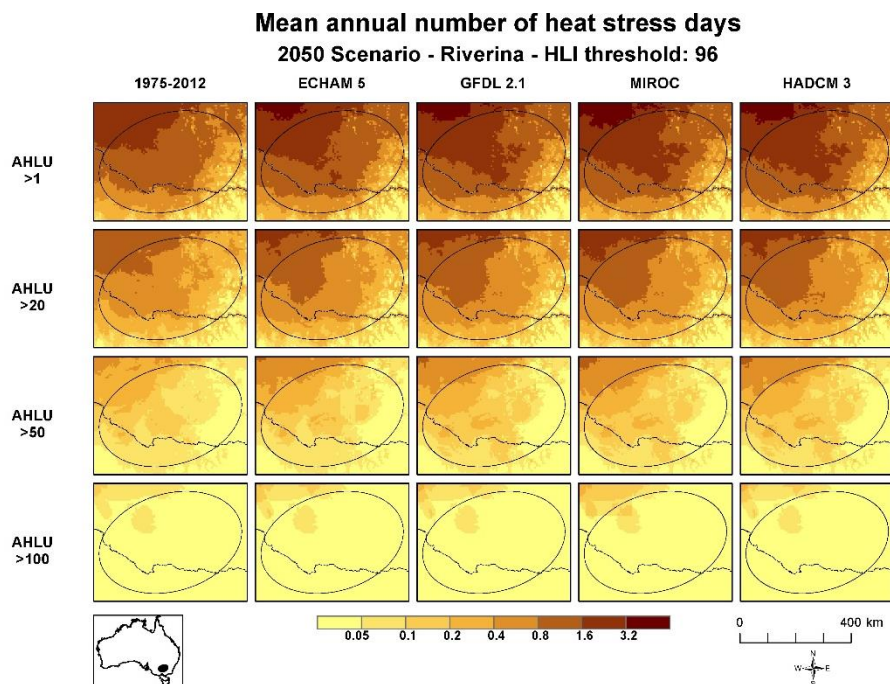


Figure 56. Riverina maps of historical (1975-2012) and 2050 GCM scenarios showing mean of number of heat stress days per year for cattle with HLI upper limit of 96.

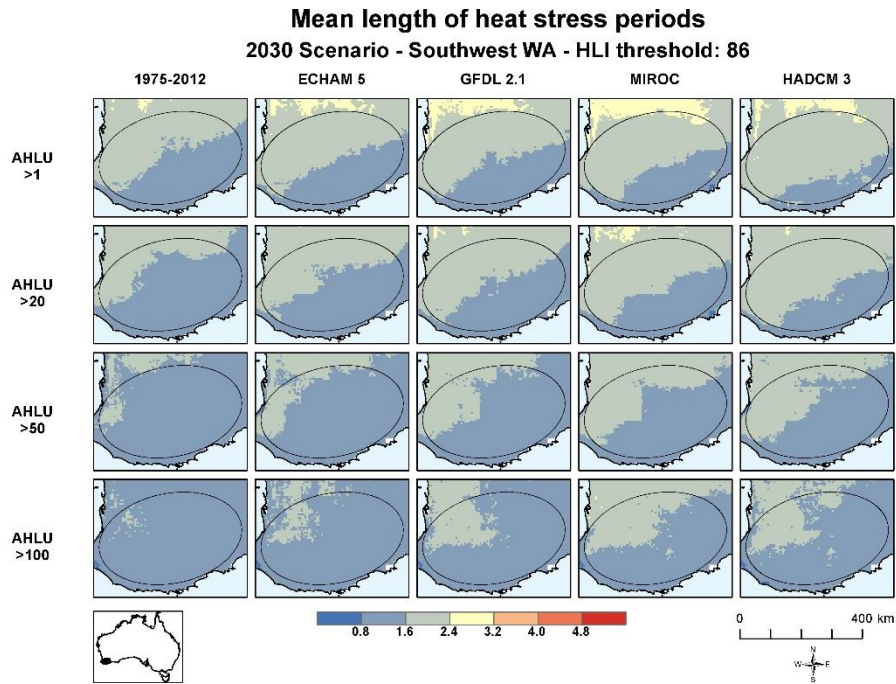


Figure 57. Southwest Western Australia maps of historical (1975-2012) and 2030 GCM scenarios showing mean of length of consecutive periods of heat stress for cattle with HLI upper limit of 86.

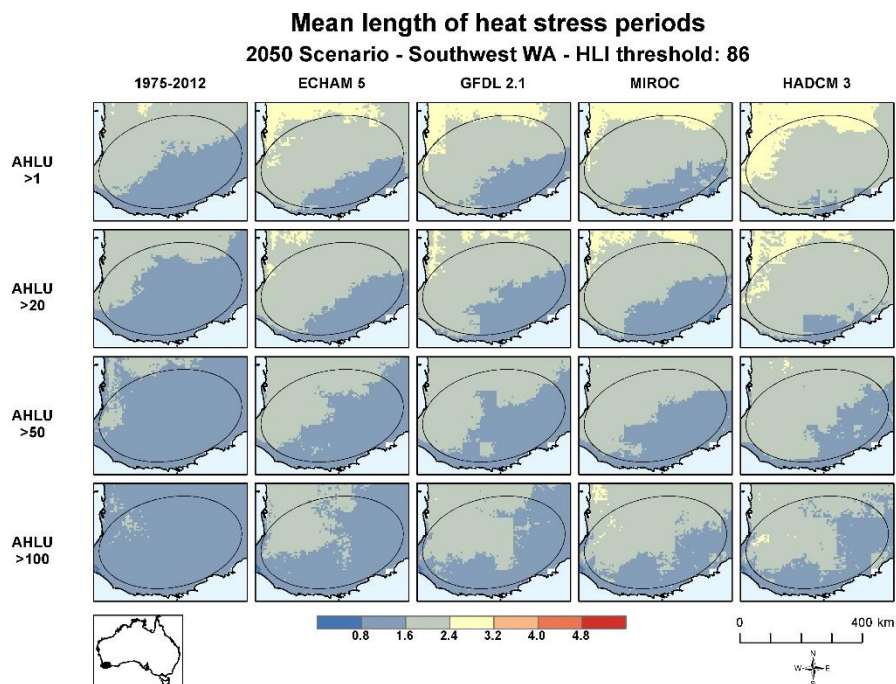


Figure 58. Southwest Western Australia maps of historical (1975-2012) and 2050 GCM scenarios showing mean of length of consecutive periods of heat stress for cattle with HLI upper limit of 86.

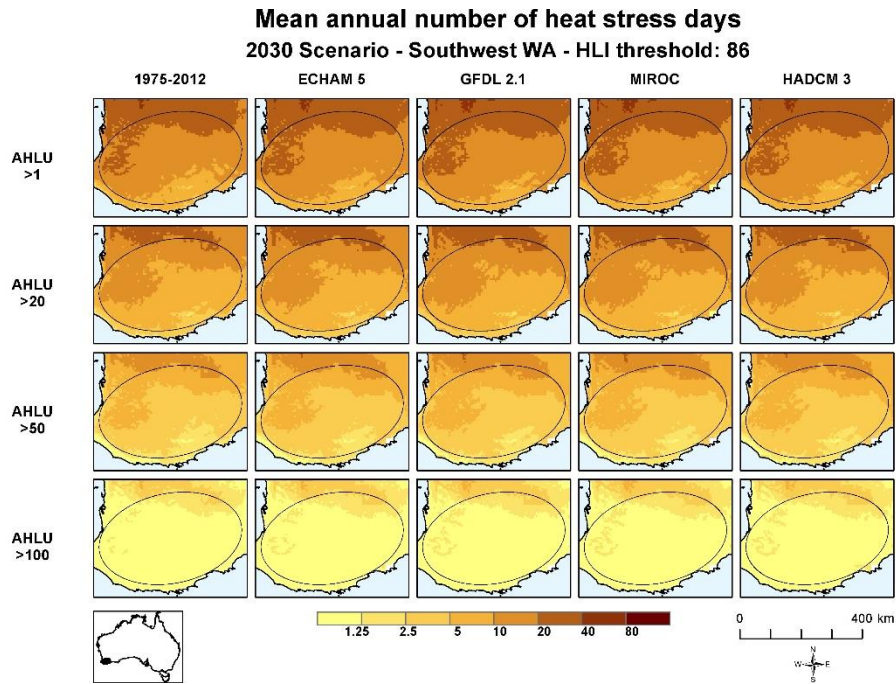


Figure 59. Southwest Western Australia maps of historical (1975-2012) and 2030 GCM scenarios showing mean of number of heat stress days per year for cattle with HLI upper limit of 86.

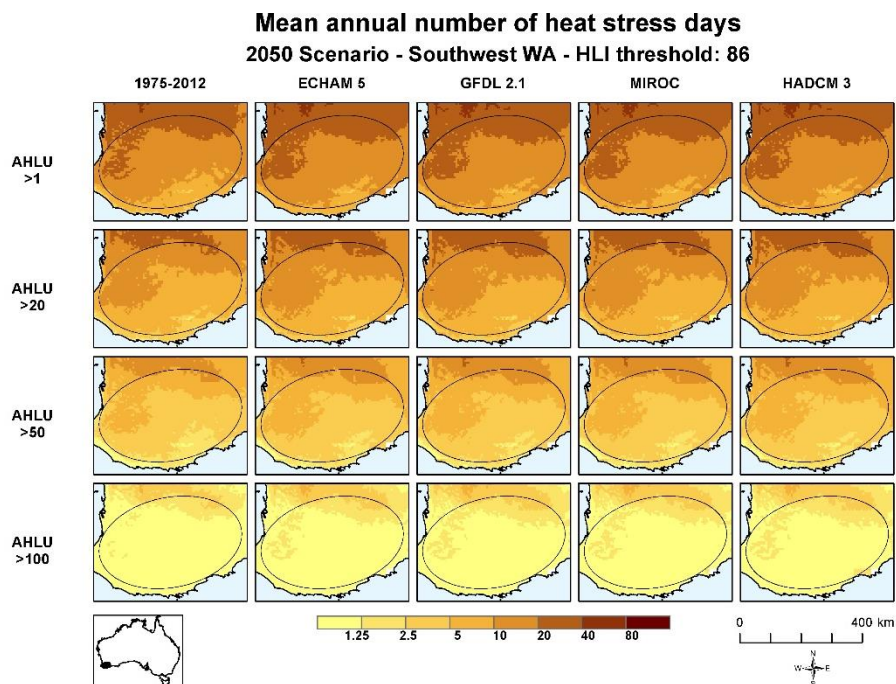


Figure 60. Southwest Western Australia maps of historical (1975-2012) and 2050 GCM scenarios showing mean of number of heat stress days per year for cattle with HLI upper limit of 86.

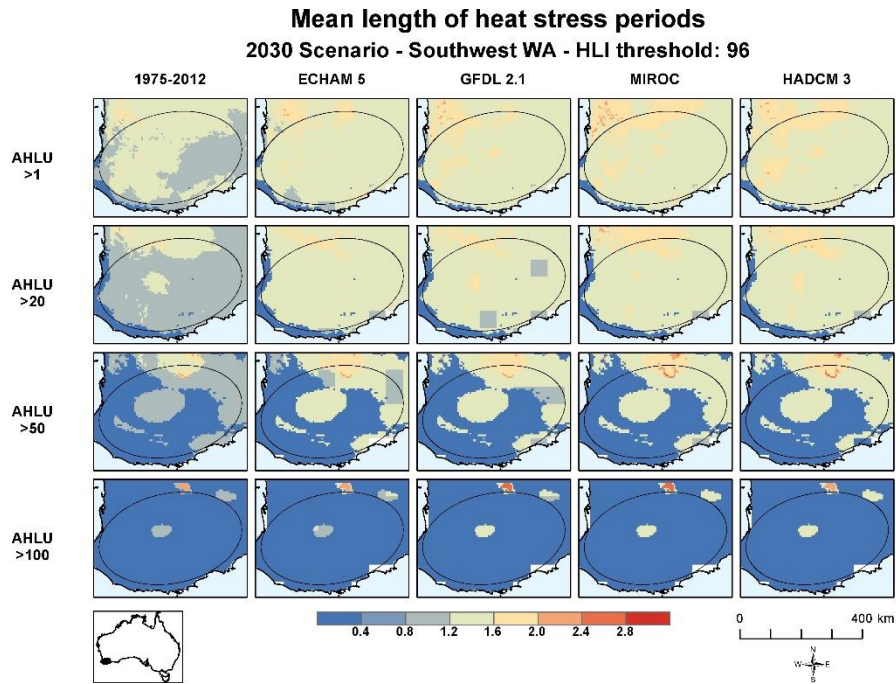


Figure 61. Southwest Western Australia maps of historical (1975-2012) and 2030 GCM scenarios showing mean of length of consecutive periods of heat stress for cattle with HLI upper limit of 96.

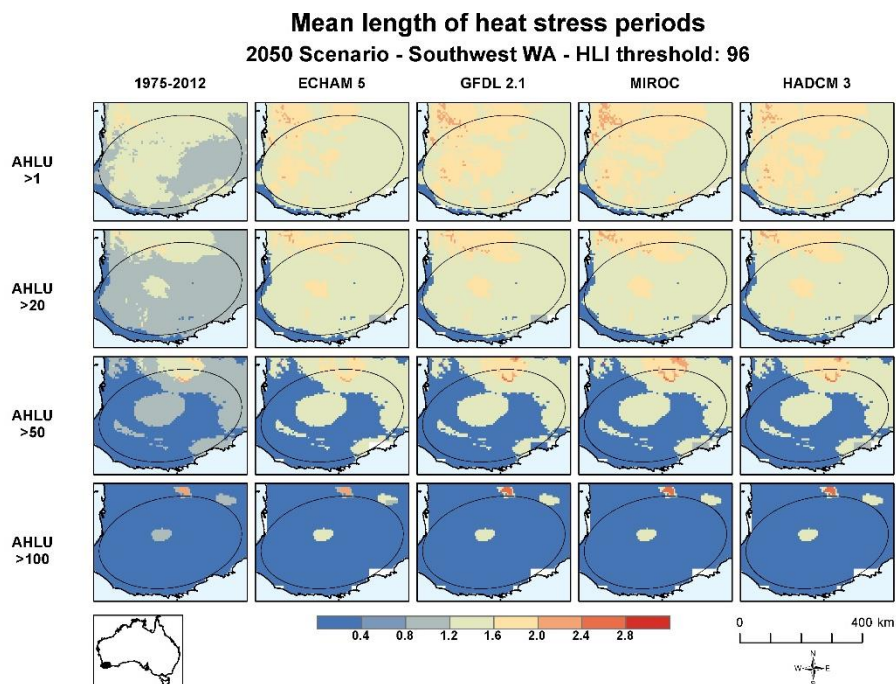


Figure 62. Southwest Western Australia maps of historical (1975-2012) and 2050 GCM scenarios showing mean of length of consecutive periods of heat stress for cattle with HLI upper limit of 96.

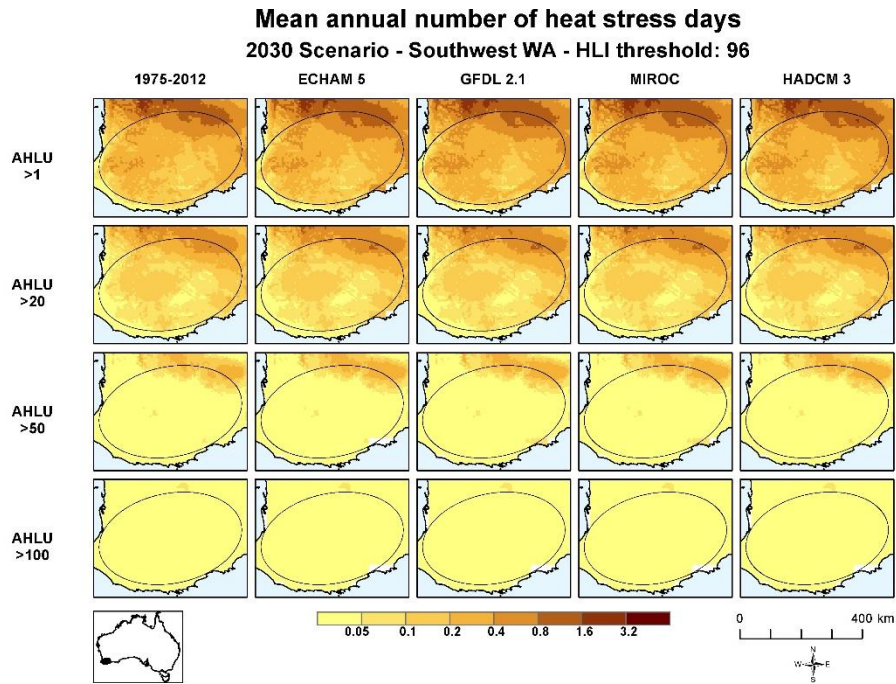


Figure 63. Southwest Western Australia maps of historical (1975-2012) and 2030 GCM scenarios showing mean of number of heat stress days per year for cattle with HLI upper limit of 96.

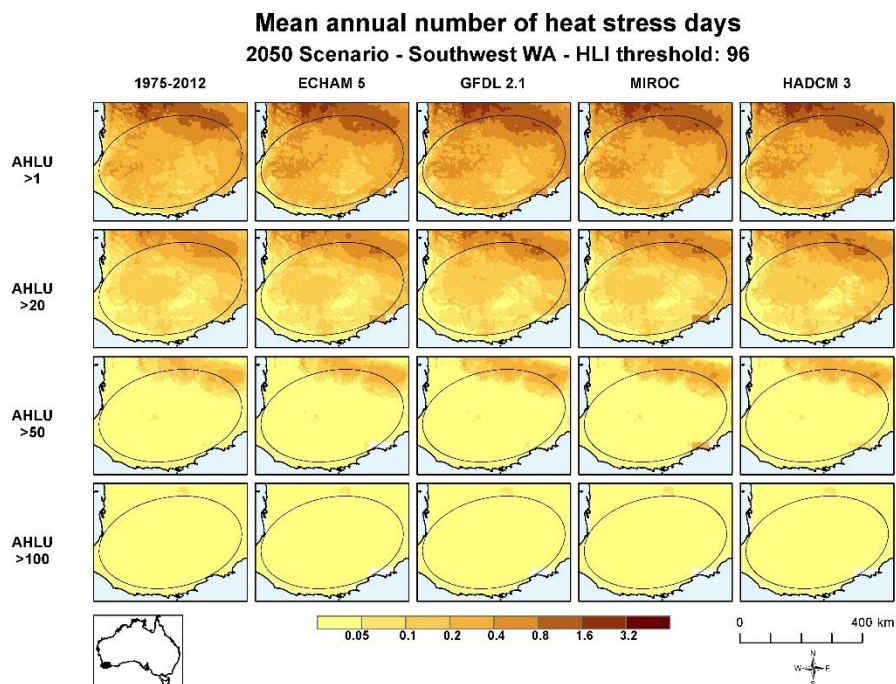


Figure 64. Southwest Western Australia maps of historical (1975-2012) and 2050 GCM scenarios showing mean of number of heat stress days per year for cattle with HLI upper limit of 96.